INCT-FNA
INSTITUTO NACIONAL DE CIÊNCIA E TECNOLOGIA
FÍSICA NUCLEAR E APLICAÇÕES

NUMEN

INSTITUTO DE FÍSICA
Universidade Federal Fluminense

Two-proton transfer reactions in the 18O+40Ca and 20Ne+116Cd collisions

Jonas L. Ferreira

Institute of Physics
Federal Fluminense University
jonasleonardo@id.uff.br

CAPES CNPq FAPERJ

Main Goals

- Two-particle transfer is a very good tool to study the correlations of both transferred particles in the transfer reaction.
  - ✓ Sequential and direct mechanisms are involved.

  $^{18}O+^{12,13}C$, $^{18}O+^{16}O$, $^{18}O+^{28}Si$, $^{18}O+^{64}Ni$
- Transfer reactions can be a contaminant in collisions where double charge Exchange cross sections are measured.

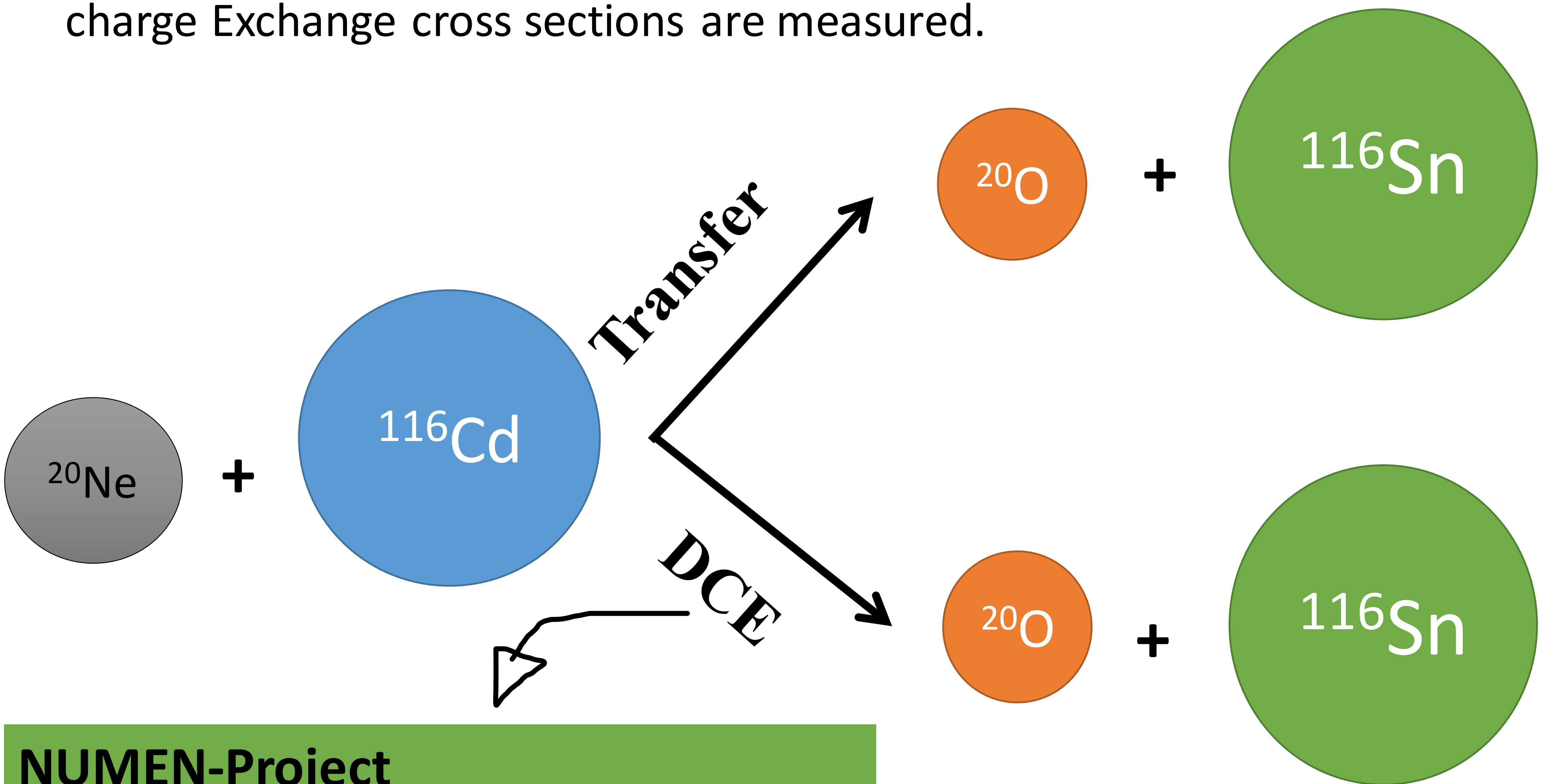

NUMEN-Project

F. Cappuzzello et al., Eur. Phys. J. A (2018) 54: 72

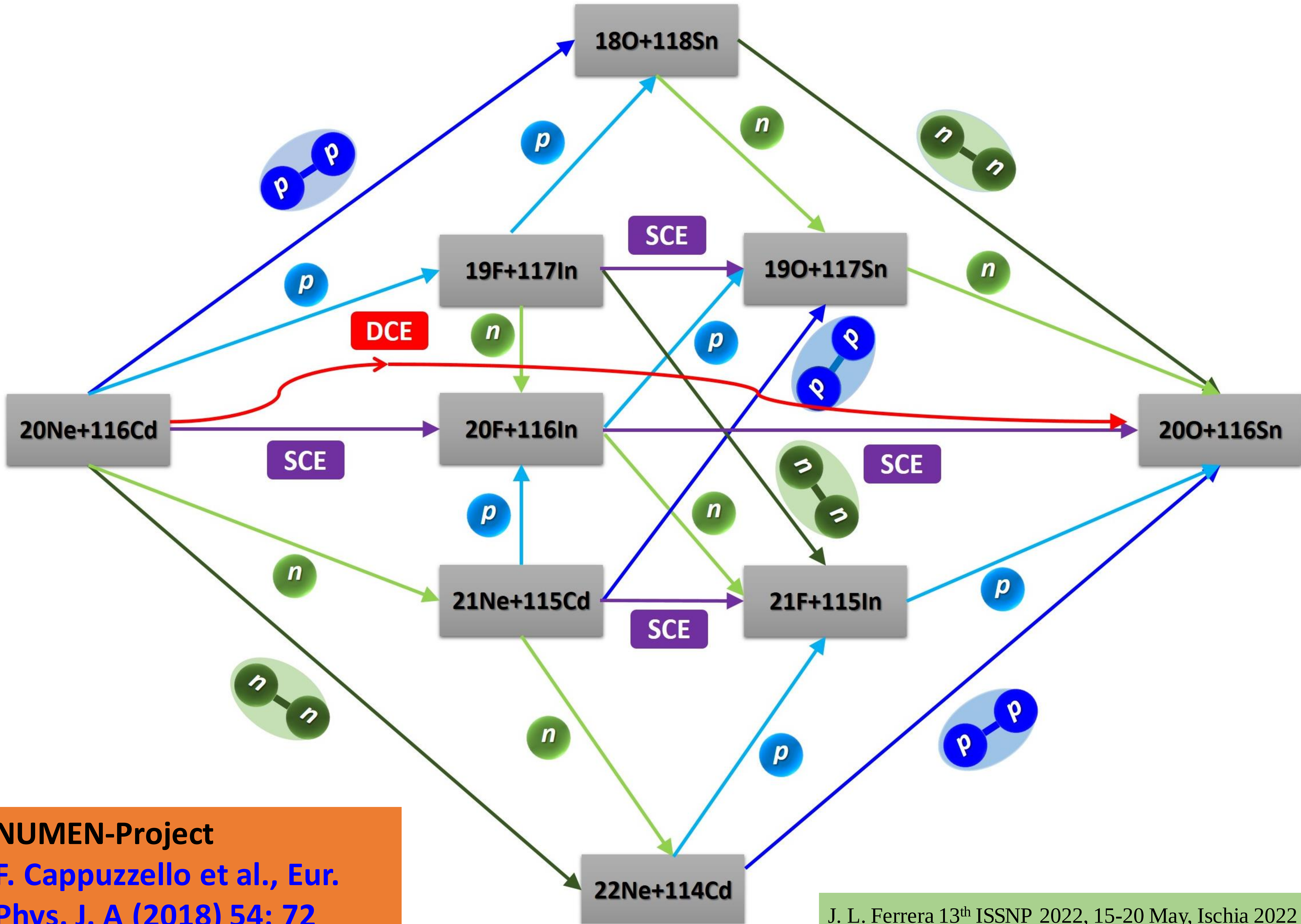

NUMEN-Project
F. Cappuzzello et al., Eur. Phys. J. A (2018) 54: 72

Theoretical models and main ingredients

$$T_{\alpha\beta}^{Direct} = \langle \psi_\beta{}^{(-)} | W_\alpha | \psi_\alpha{}^{(+)} \rangle$$

$$\Phi_{I_a}(\xi_a) = \sum A_{j_1 j_2 j_{12}}^{j_{12} I_b I_a} \left[\Phi_{I_b}(\xi_b) \times [\varphi_{j_1}(\boldsymbol{r}_1) \times \varphi_{j_2}(\boldsymbol{r}_2)]_{j_{12}} \right]_{I_A}$$

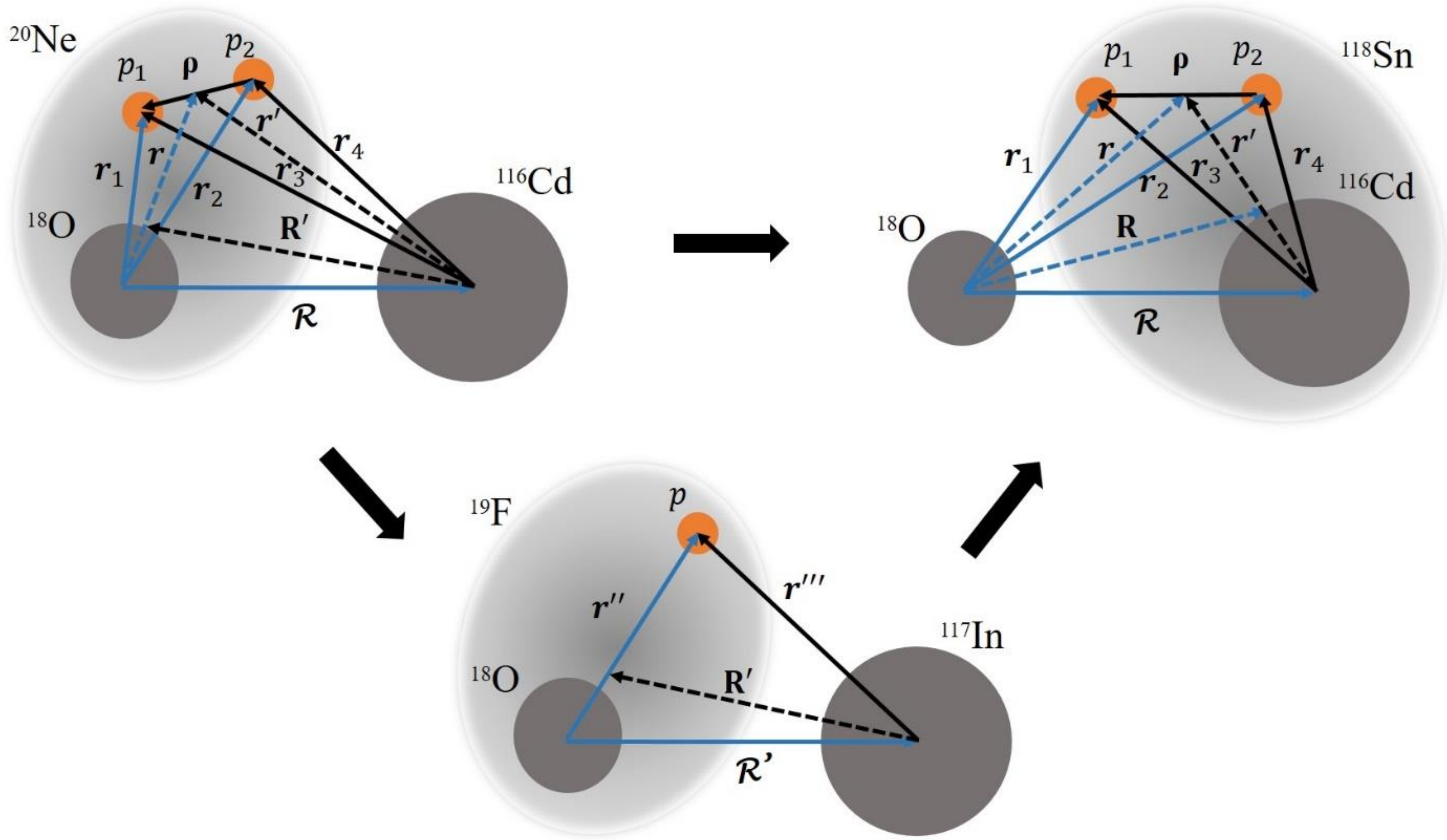

- ✓ **Fresco code – I. Thompson;**
- ✓ **DWBA, CCBA and CRC calculations;**
- ✓ **Woods-Saxon potential are used to generate the single-particle wave functions;**
- ✓ **São Paulo potential is used in each partition;**
- ✓ **Spectroscopic amplitudes**

$$T_{\alpha\beta}^{seq} = \sum_\gamma \langle \psi_\beta{}^{(-)} | W_\gamma | \phi_\gamma \rangle \tilde{G}_\gamma^{(+)} \langle \phi_\gamma | W_\alpha | \psi_\alpha{}^{(+)} \rangle - \langle \psi_\beta{}^{(-)} | \phi_\gamma \rangle \langle \phi_\gamma | W_\alpha | \psi_\alpha{}^{(+)} \rangle$$

$$\Phi_a(\xi_a) = \sum_{lsj} A_{lsj}^{j I_b I_a} [\Phi_{I_b}(\xi_b) \times \varphi_{lsj}(\boldsymbol{r})]_{I_a}$$

Theoretical models and main ingredients

- *São Paulo Potential*

  L. C. Chamon, et al. Phys. Rev. Lett. 79, 5218 (1997)

  L. C. Chamon, et al. Phys. Rev. C. 66, 014610 (2002)

- $U(R) = (1.0 + 0.78i)V_{LE}^{SP}(R)$ *intermediate and final partition*

  L. R. Gasques, et. al., Nucl. Phys. A 764, 135 (2006)

- $U(R) = (1.0 + 0.6i)V_{LE}^{SP}(R)$ *initial partition*

  D. Pereira et al. PLB 670, 330 (2009)

$$V_{LE}^{SP} = V_F(\boldsymbol{R})e^{4v^2/c^2}$$

$$V_F = \int \rho_1(\boldsymbol{r}_1)\mathcal{V}(\boldsymbol{R} - \boldsymbol{r}_1 + \boldsymbol{r}_2)\rho_2(\boldsymbol{r}_2)\, d\boldsymbol{r}_1 \mathrm{d}\boldsymbol{r}_2$$

$\mathcal{V}(\boldsymbol{R} - \boldsymbol{r}_1 + \boldsymbol{r}_2)$ *is the known nucleon − nucleon M3Y interaction*

$$\rho(r) = \frac{\rho_0}{1 + e^{(r-R_0)/a}}$$

$$R_0 = \left(1.31A^{1/3} - 0.84\right) fm$$

$$a = 0.56\ fm$$

2p-transfer stripping reaction in the 20Ne+116Cd collision at 306 MeV

Structure calculation

❑ **Shell Model**

➢ **Ligther nuclei**

✓ **Interaction: p-sd-mod (4He as core)**

✓ Y. Utsuno and S. Chiba, Phys. Rev. C 83, 021301(R) (2001)

➢ **Heavy nuclei**

✓ **Interaction: jj45pna**

✓ R. Machleidt, Phys. Rev. C **63**, 024001 (2001).

✓ **Model Space**

protons – 1f5/2, 2p3/2, 2p1/2 e 1g9/2

neutrons – 1g7/2, 2d5/2, 2d3/2, 3s1/2 e 1h11/2

78Ni as core

✓ **Interaction: 88Sr45**

✓ L. Coraggio, A. Gargano, and N. Itaco, Phys. Rev. C **93**, 064328 (2016)

✓ **Model Space**

protons – 2p1/2, 1g9/2, 1g7/2 e 2d5/2

neutrons – 1g7/2, 2d5/2, 2d3/2, 3s1/2 e 1h11/2

88Sr as core

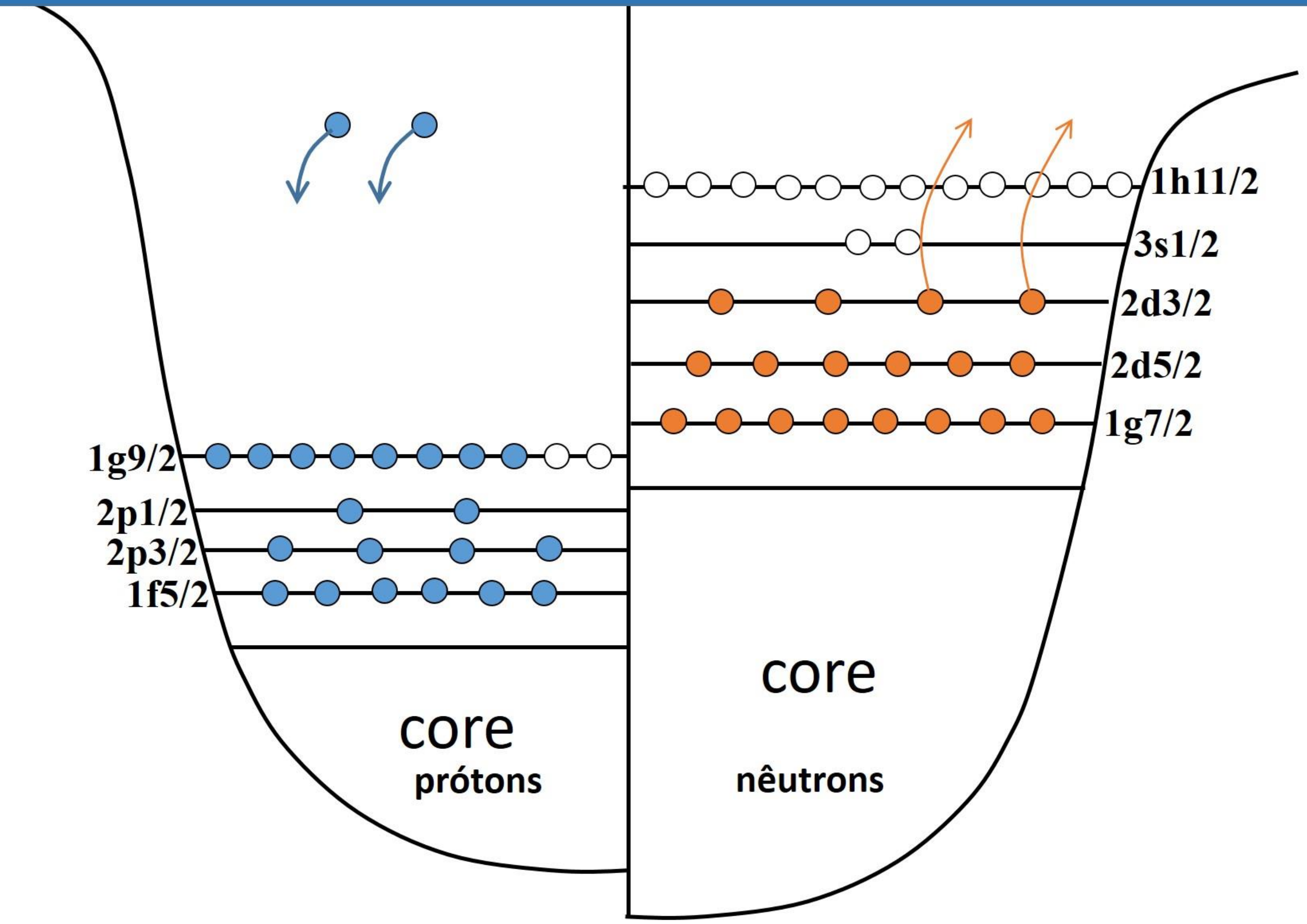

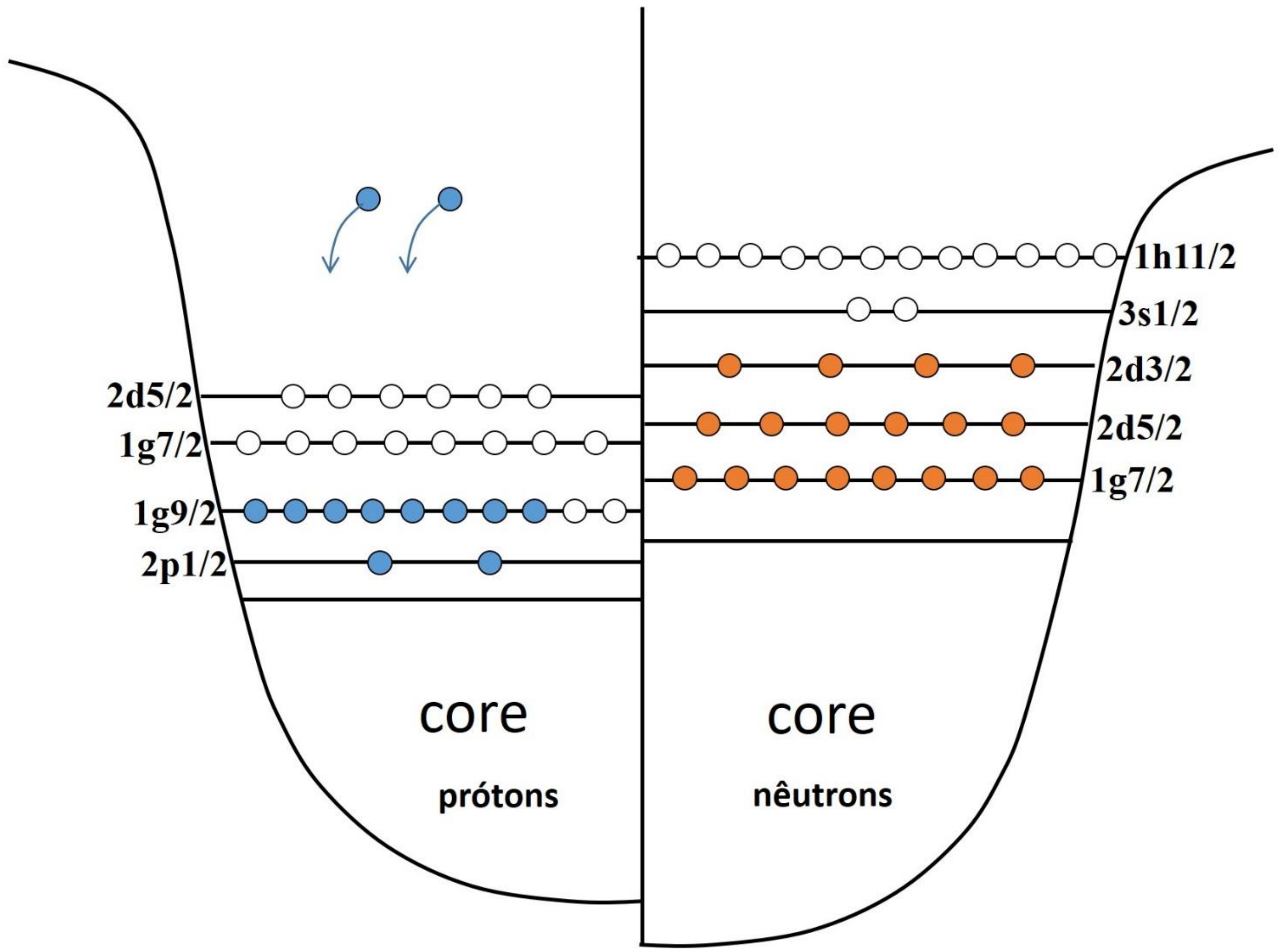

2p-transfer stripping reaction in the 20Ne+116Cd collision at 306 MeV

^{116}Cd(^{20}Ne,^{18}O)^{118}Sn

- **D. Carbone et al., Phys. Rev C 102, 044606 (2020)**

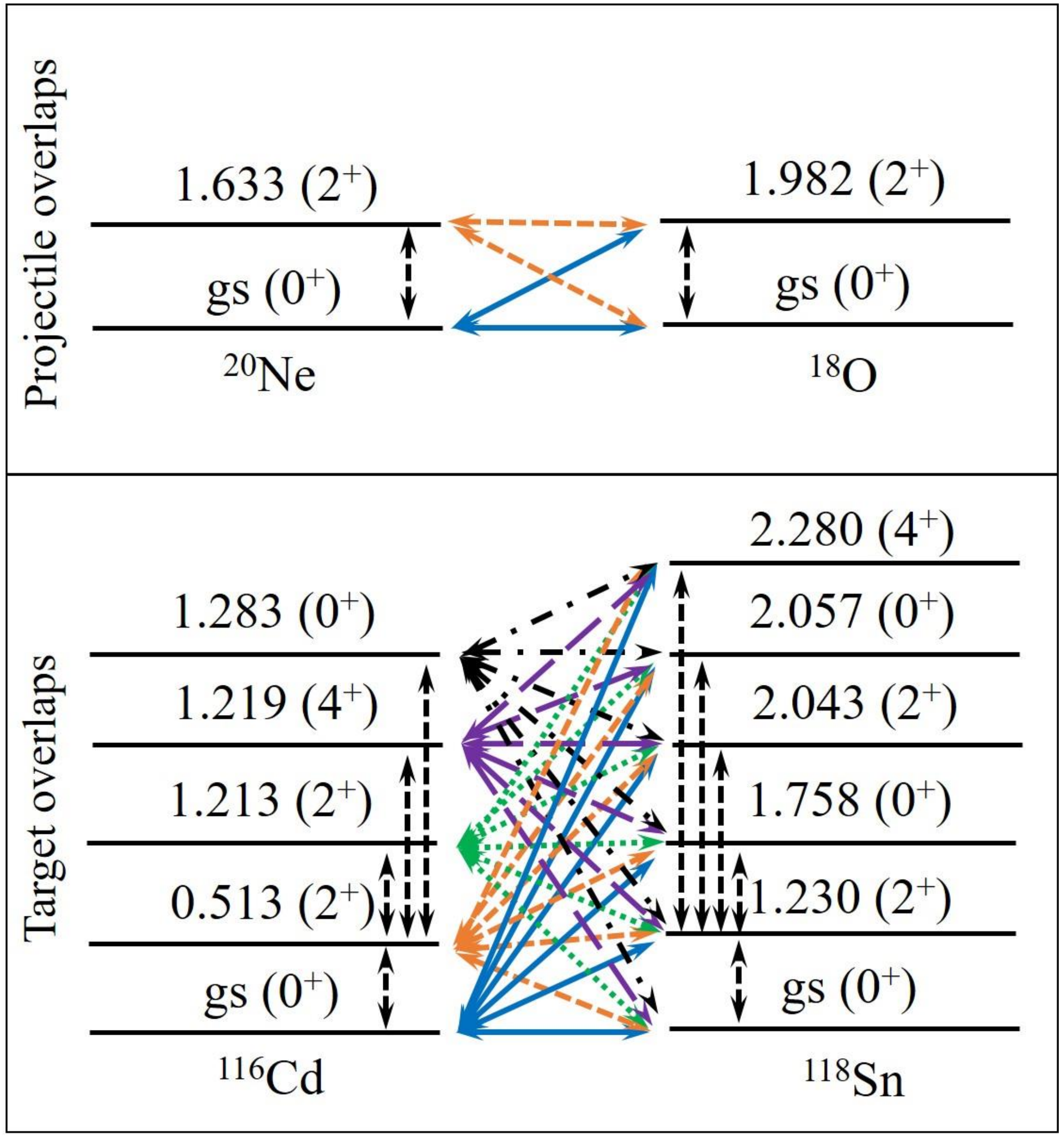

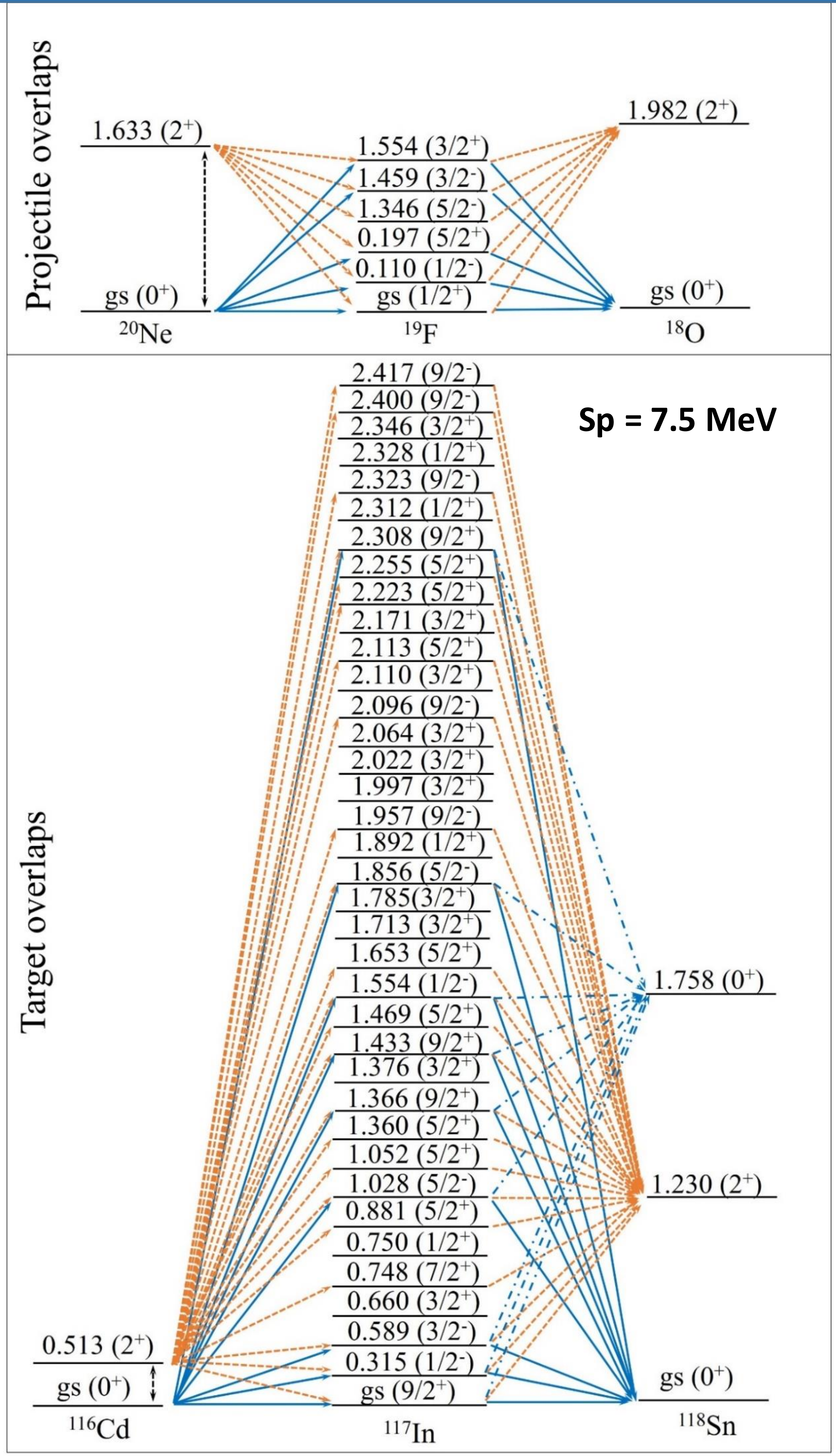

2p-transfer stripping reaction in the 20Ne+116Cd collision at 306 MeV

		jj45pna				88Sr45	
Final channel	Exp.	IC-1 (nb)	Seq-1 (nb)	IC-2 (nb)	Seq-2 (nb)	IC-2 (nb)	Seq-2 (nb)
${}^{18}O_{gs}(0^+) + {}^{118}Sn_{gs}(0^+)$	40 ± 15	22	19.1	30.9	52.1	39.5	88.5
${}^{18}O_{gs}(0^+) + {}^{118}Sn_{1.229}(2^+)$	140 ± 60	5.3	1.6	26.9	39.8	52.7	106.3

- **D. Carbone et al., Phys. Rev C 102, 044606 (2020)**

- **IC-1 e Seq-1 – no couplings with inelastic states in the initial partition.**

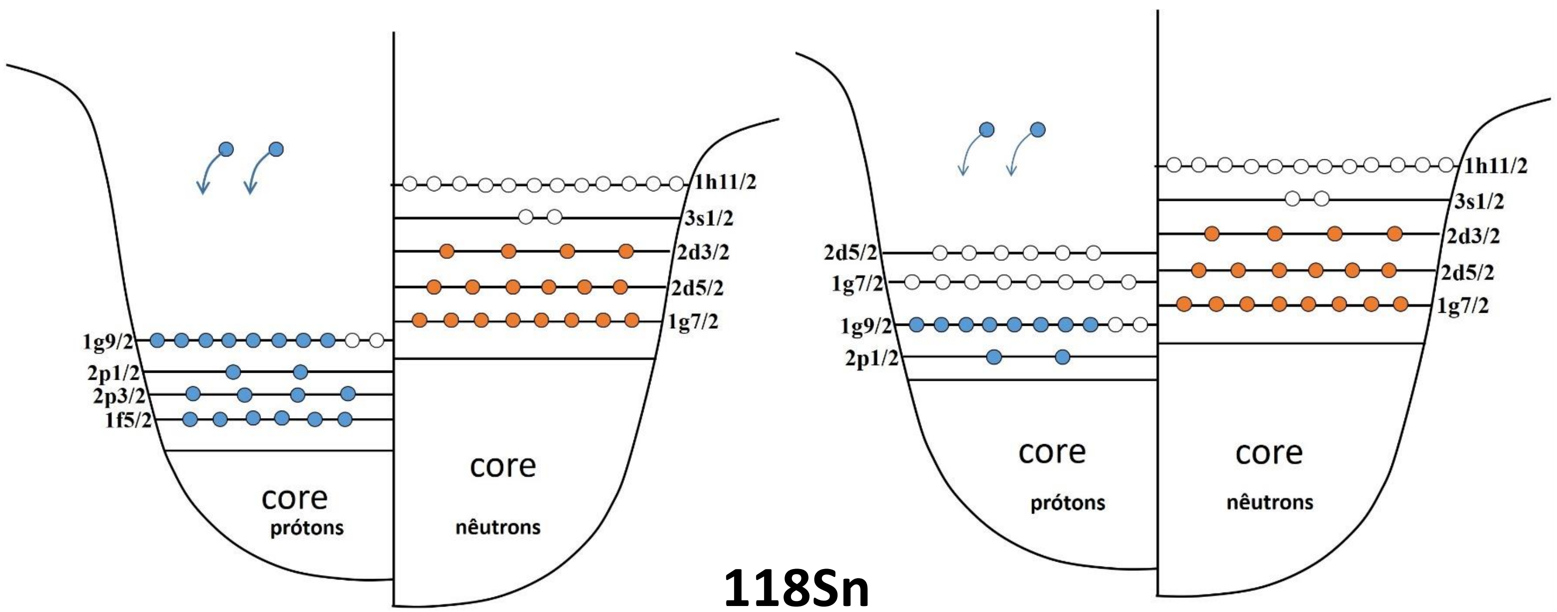

118Sn

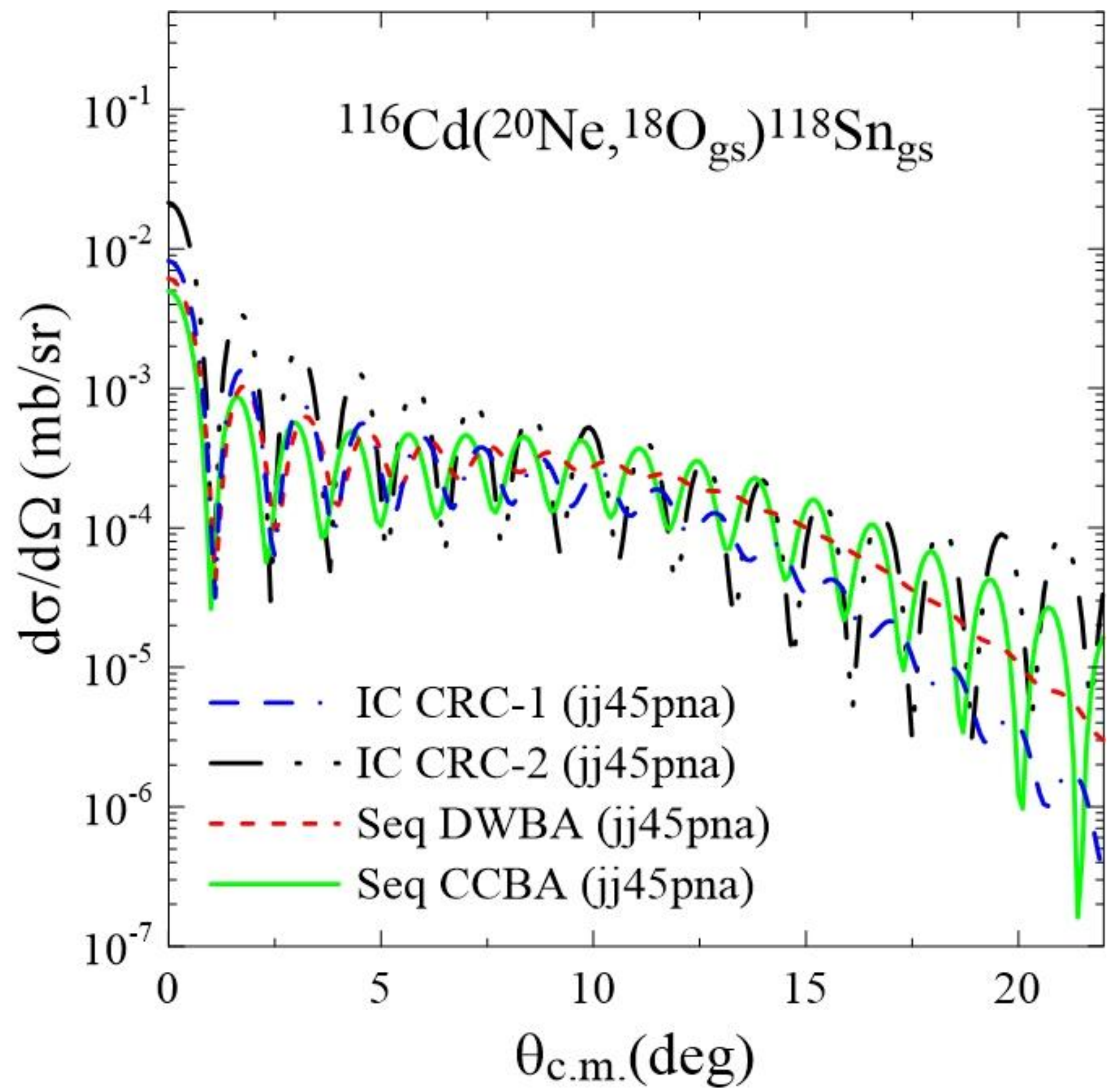

2n-transfer pickup reaction in the 20Ne+116Cd collision at 306 MeV

$^{116}Cd(^{20}Ne,^{22}Ne)^{114}Cd$

- **D. Carbone et al., Phys. Rev C 102, 044606 (2020)**

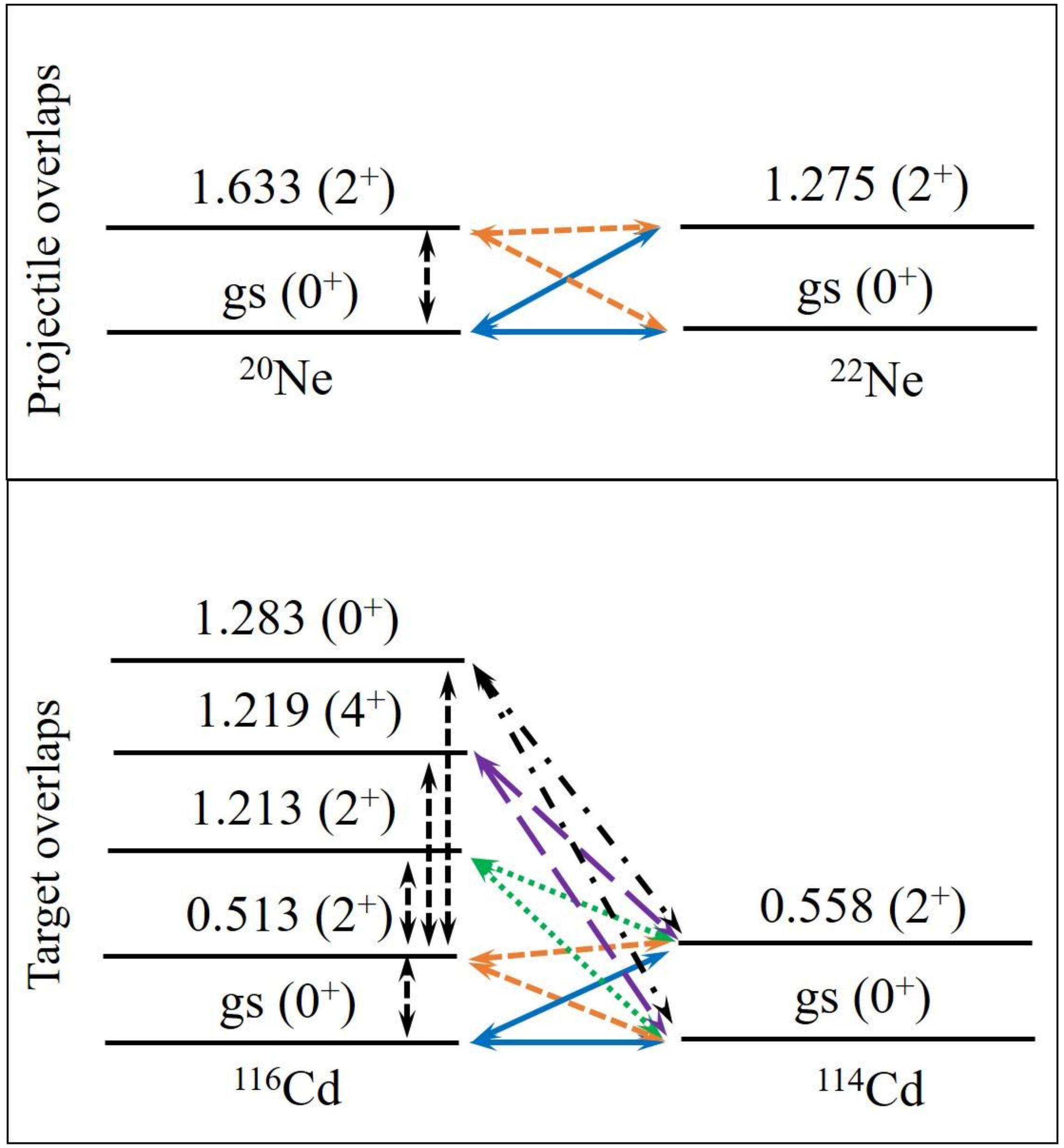

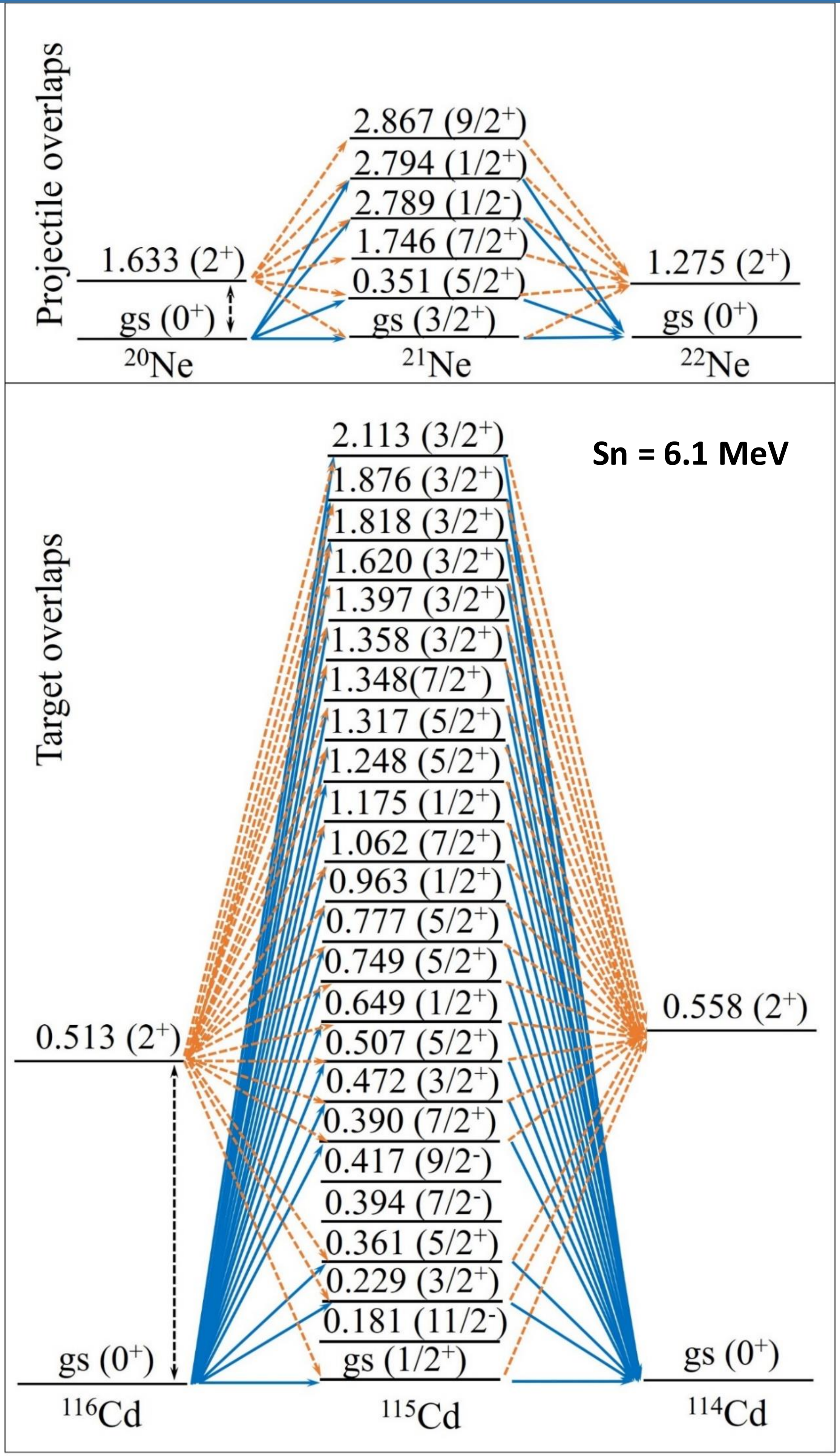

2n-transfer pickup reaction in the 20Ne+116Cd collision at 306 MeV

Final channel	Exp.	IC-1 (nb)	Seq-1 (nb)	IC-2 (nb)	Seq-2 (nb)
$^{20}Ne_{gs}(0^+) + {}^{114}Cd_{gs}(0^+)$	370 ± 190	251	613	209	427
$^{20}Ne_{gs}(0^+) + {}^{114}Cd_{0.558}(2^+)$	420 ± 190	313	721	314	636

- **D. Carbone et al., Phys. Rev C 102, 044606 (2020)**
- **IC-1 e Seq-1 – no couplings with inelastic states in the initial partition.**

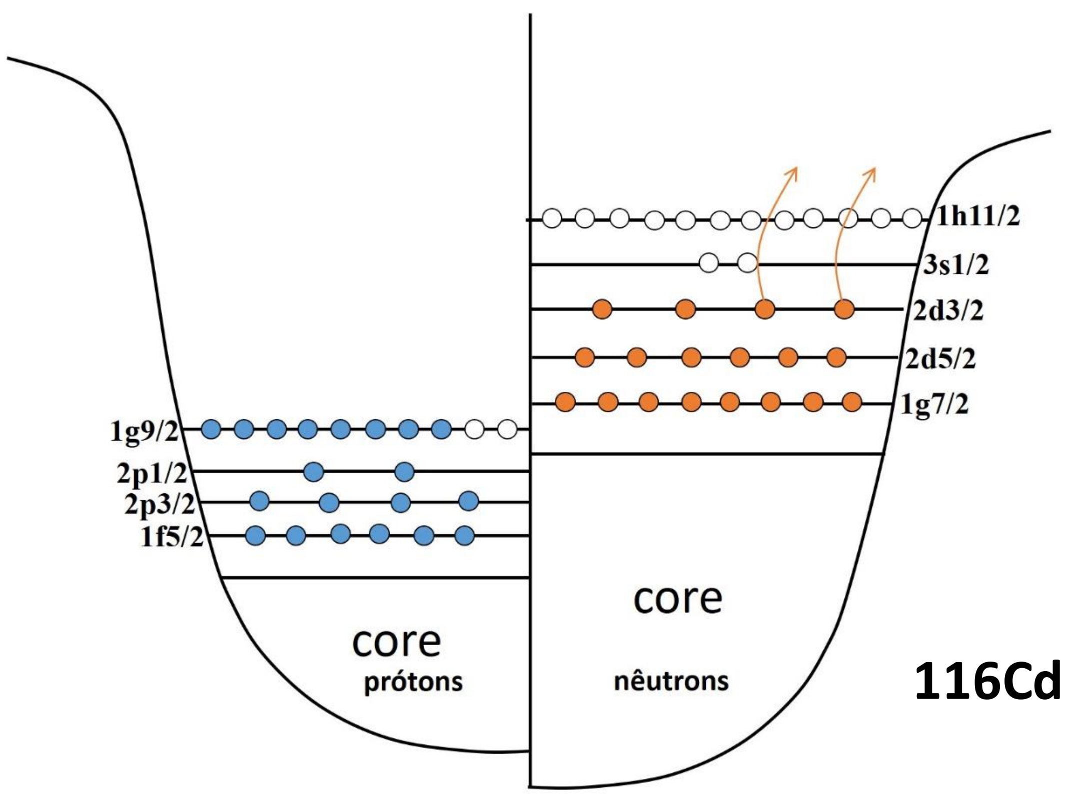

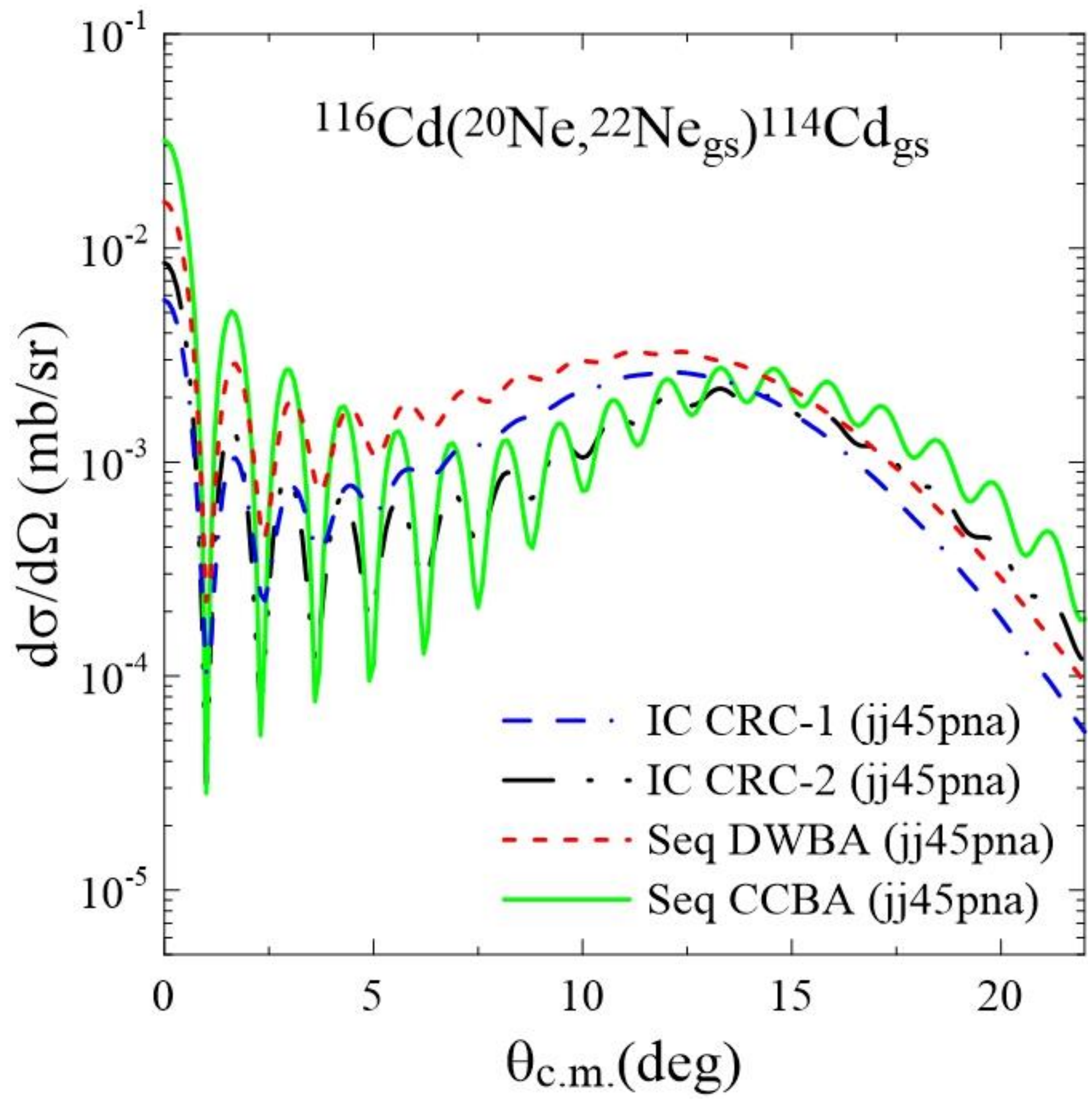

D. Carbone et al Phys. Rev. C 102, 044606 (2020)
S. Burrello et al Phys. Rev. C 105 024616 (2022);
J. L. Ferreira et al Phys. Rev. C 105 014630 (2022)

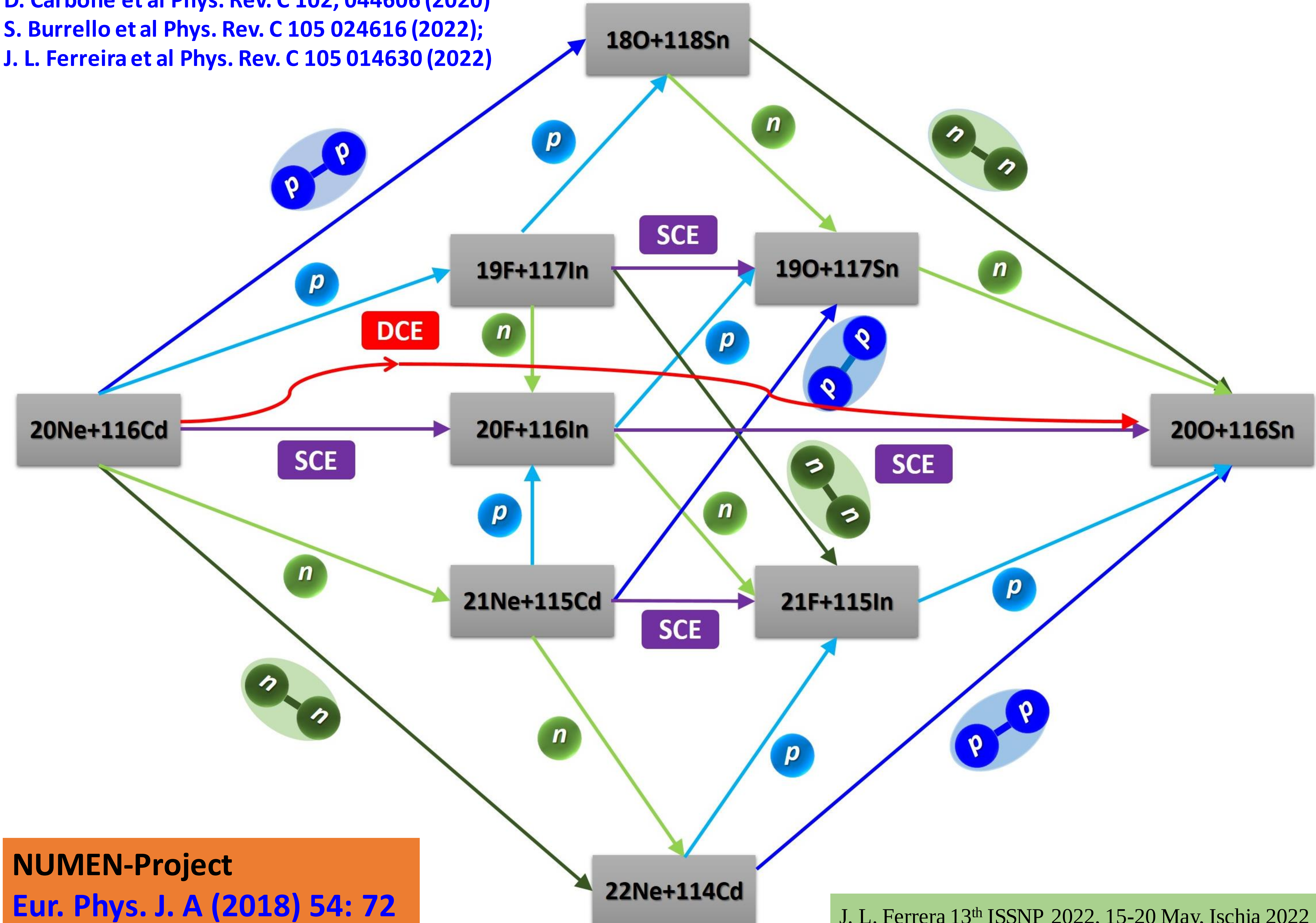

NUMEN-Project
Eur. Phys. J. A (2018) 54: 72

2p-transfer stripping reaction in the 18O+40Ca collision at 270 MeV

Spectroscopic amplitudes for the target overlaps

- ❑ **Shell Model calculations – NuShellX**

- ➢ **Efective interaction: ZBMmod**

E. Caurier *et al.*, Phys. Lett. B **522**, 240 (2001).
M. L. Bissell, et al., Phys. Rev. Lett. **113**, 052502 (2014).

- ➢ **Model Space for both protons and neutrons**

  2s1/2, 1d3/2, 1f7/2 and 2p3/2

  28Si as core

Spectroscopic amplitudes for the proj. overlaps

- ➢ **Efective interaction: ZBM**

A. P. Zuker, B. Buck, and J. B. McGrory, Phys. Rev. Lett. 21, 39 (1968).

- ➢ **Model Space for both protons and neutrons**

  1p1/2, 1d5/2 and 2s1/2

  12C as core

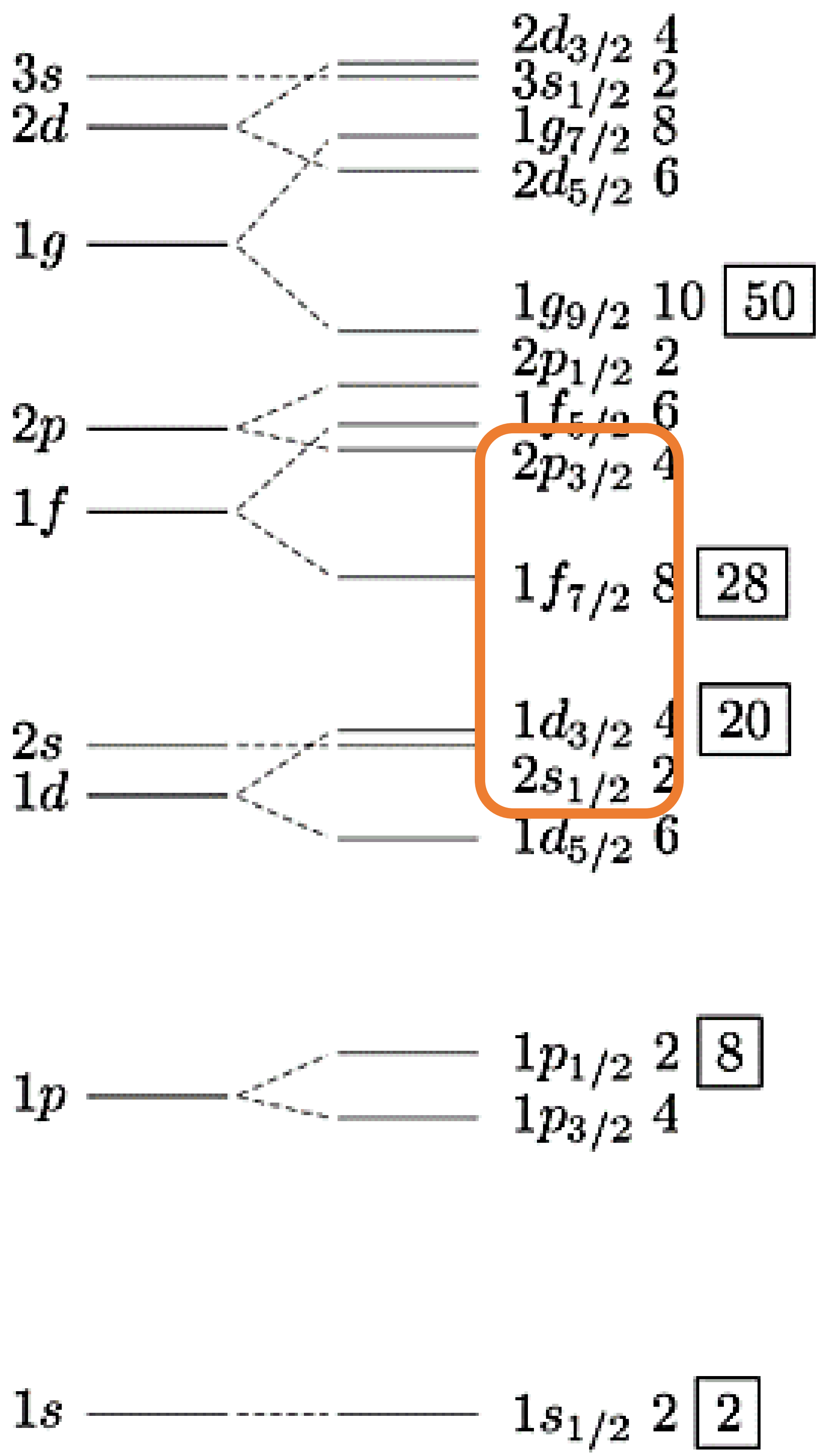

2p-transfer stripping reaction in the 18O+40Ca collision at 270 MeV

Spectroscopic amplitudes for the target overlaps

- ❑ **Shell Model calculations – NuShellX**

- ➢ **Efective interaction: ZBMmod**

E. Caurier *et al.*, Phys. Lett. B **522**, 240 (2001).

M. L. Bissell, et al., Phys. Rev. Lett. **113**, 052502 (2014).

- ➢ **Model Space for both protons and neutrons**

  2s1/2, 1d3/2, 1f7/2 and 2p3/2

  28Si as core

Spectroscopic amplitudes for the proj. overlaps

- ➢ **Efective interaction: ZBM**

A. P. Zuker, B. Buck, and J. B. McGrory, Phys. Rev. Lett. 21, 39 (1968).

- ➢ **Model Space for both protons and neutrons**

  1p1/2, 1d5/2 and 2s1/2

  12C as core

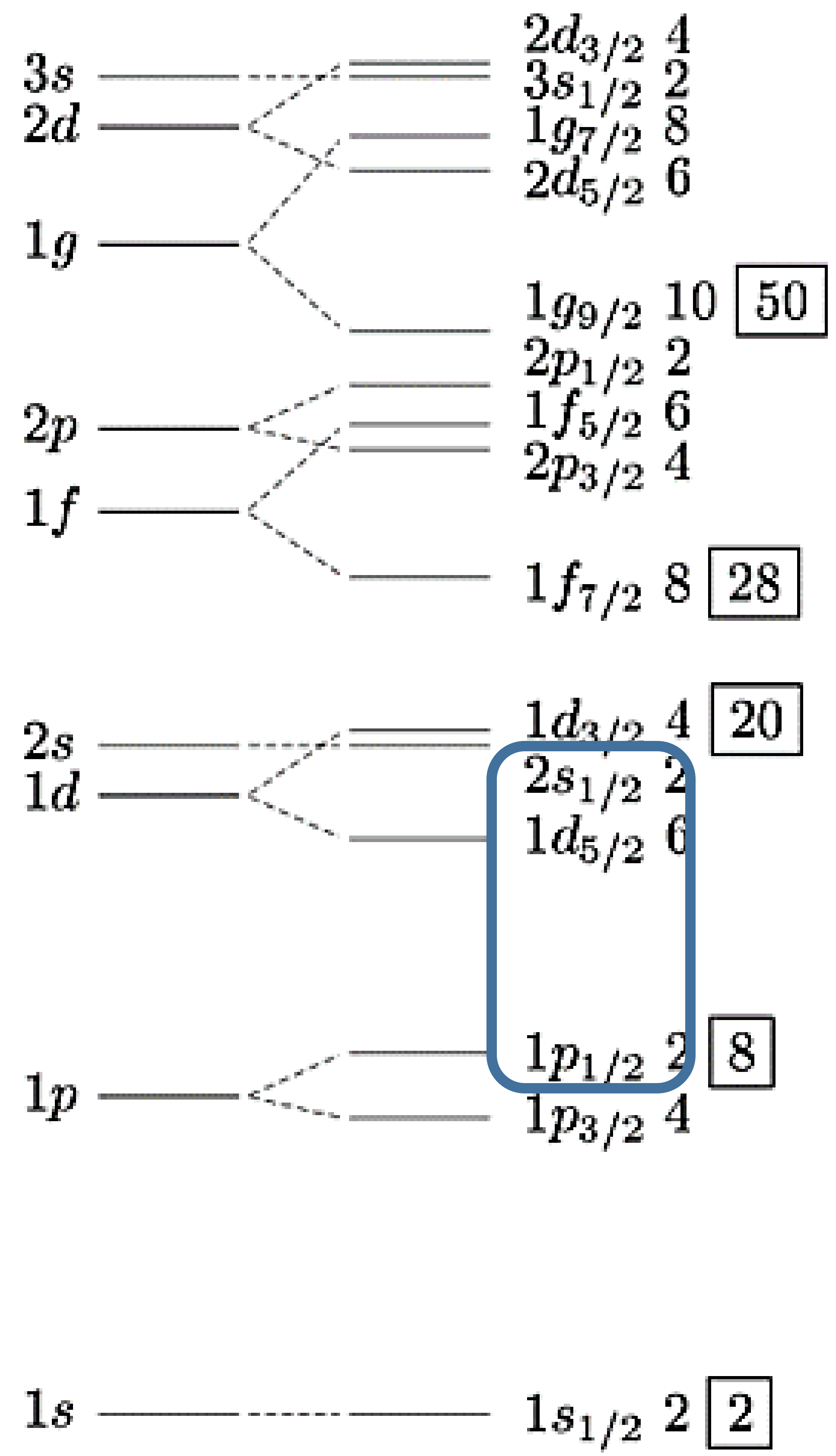

2p-transfer stripping reaction in the 18O+40Ca collision at 270 MeV

- **J. L. Ferreira et al., Phys. Rev C 103, 054604 (2021)**

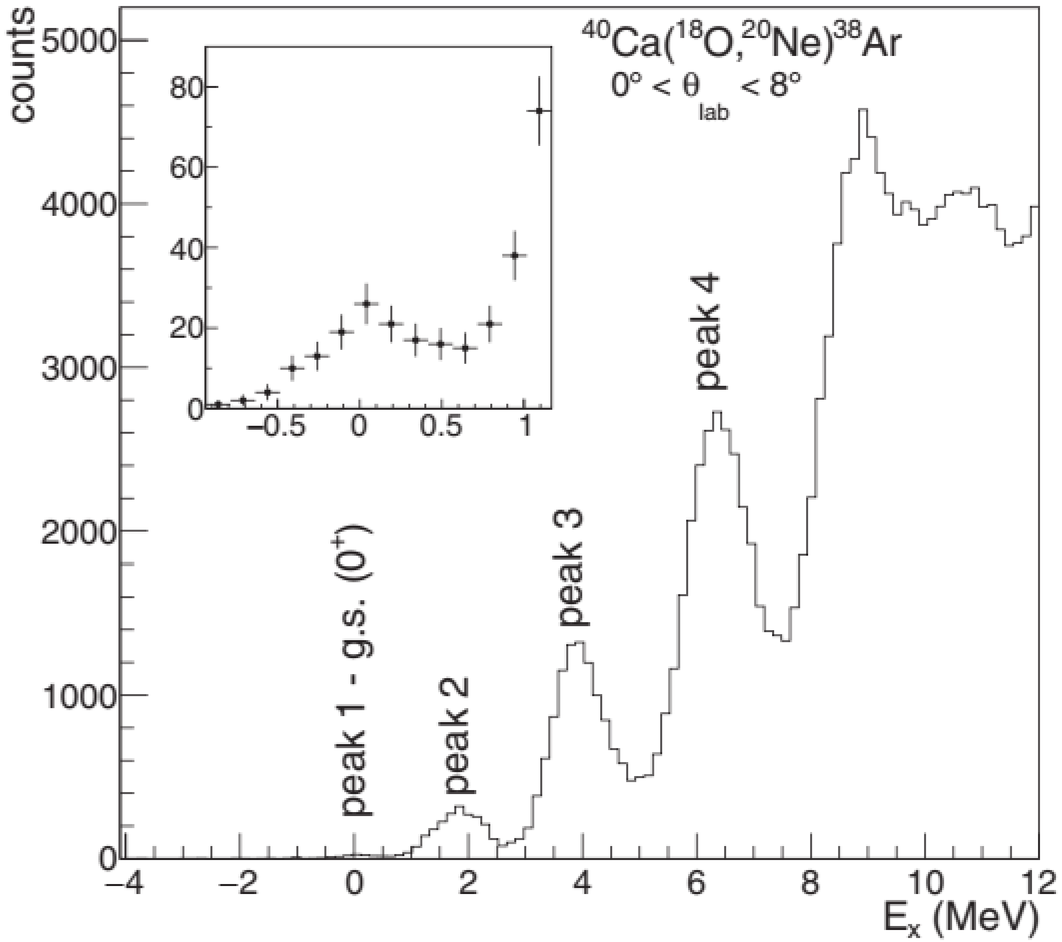

FIG. 1. Excitation energy spectrum for the ^{40}Ca(^{18}O, ^{20}Ne) ^{38}Ar reaction at 270 MeV in the angular range of 0° < θ_{lab} < +8°. In the inset a zoomed view of the ground-state region is shown.

Couplings for direct two-proton transfer

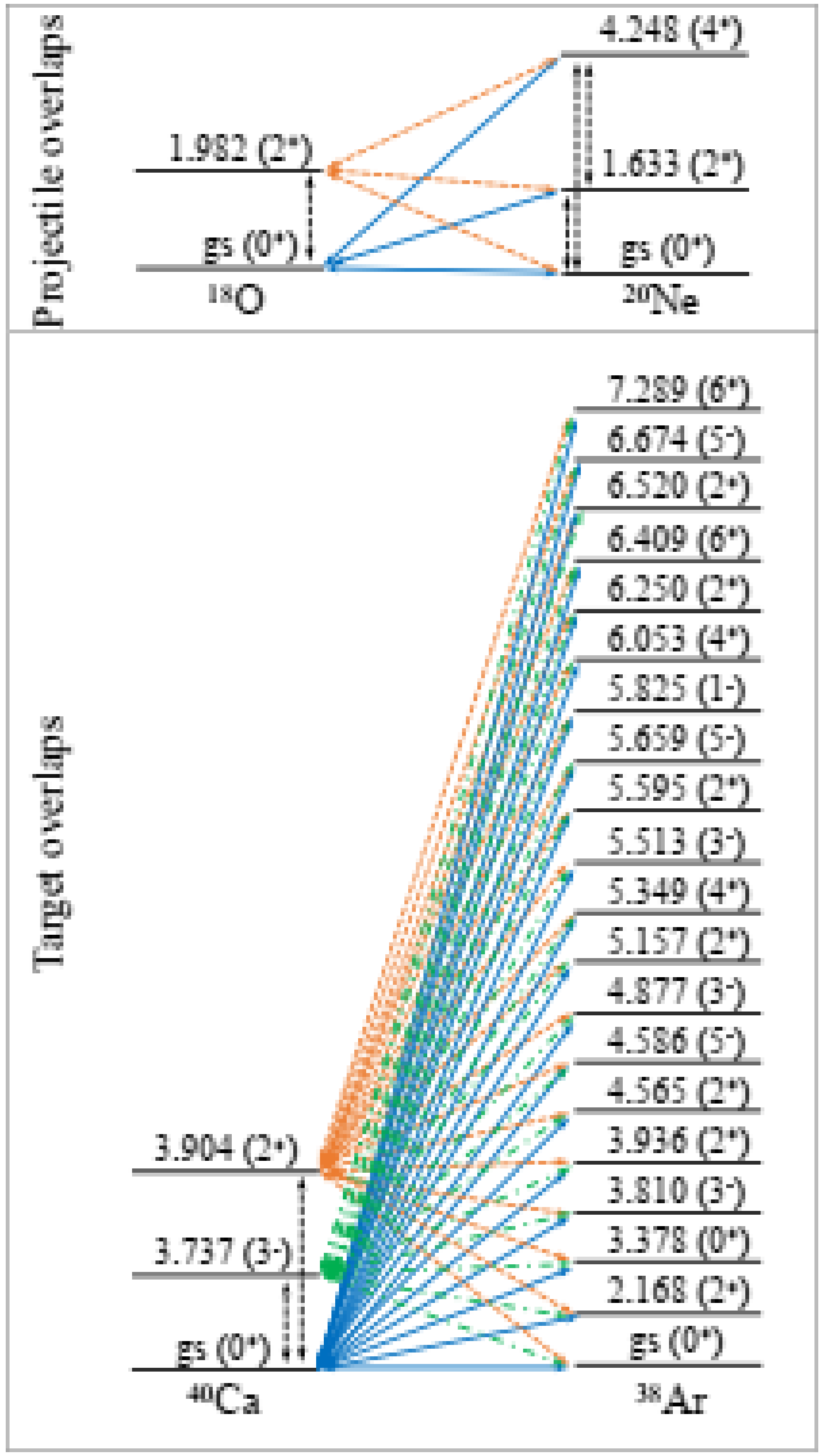

Couplings for sequential two-proton transfer

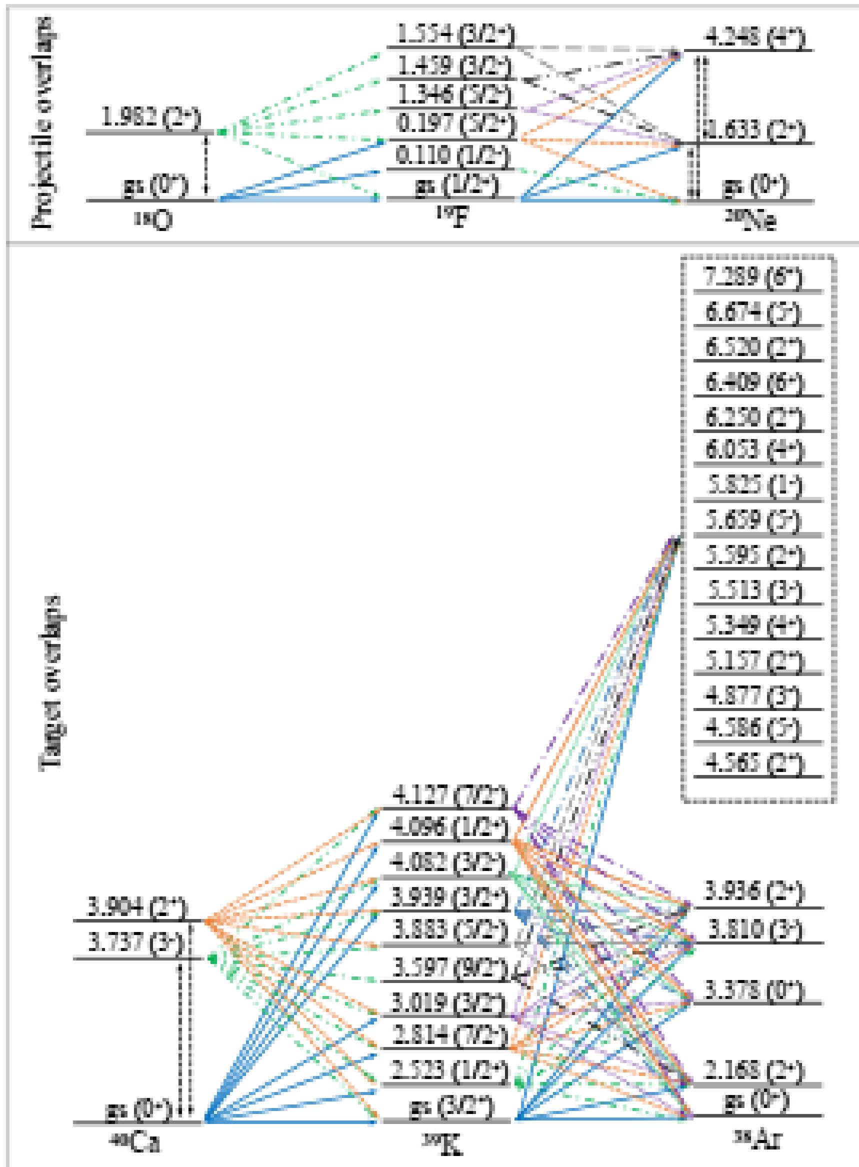

2p-transfer stripping reaction in the 18O+40Ca collision at 270 MeV

- J. L. Ferreira et al., Phys. Rev C 103, 054604 (2021)

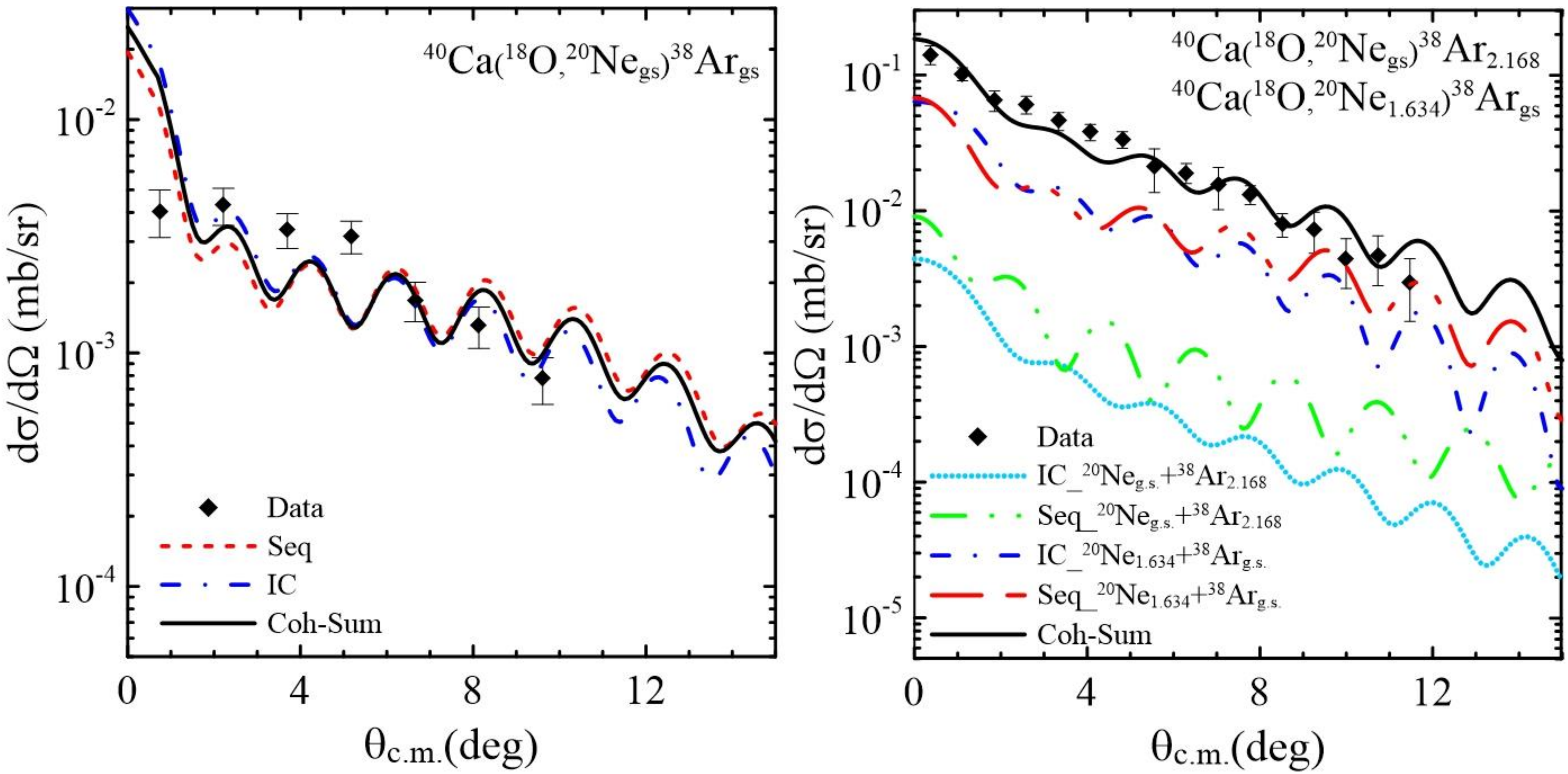

Conclusions and outlooks

- *Direct and sequential two-proton transfer mechanisms compete with each other populating the ground states of both 20Ne+38Ar and 18O+118Sn in final partition.*

- *The first 2+ excited states in the final partition are preferably populated by sequential mechanism.*

- *Couplings with inelastic states are important to be taken into account in the initial partition.*

- *The orbits above the 1g9/2 (proton model space) play a relevant role in the transfer reaction for the 20Ne+116Cd collision.*

- *Next step is to analyse two-proton transfer in the 76Ge(20Ne ,18O)78Se and the multinuceon transfer reaction in the 40Ca(18O,18Ne)40Ar*

Working group

NUMEN collaboration

F. Cappuzzello[1,2,a], C. Agodi[2], M. Cavallaro[2], D. Carbone[2], S. Tudisco[2], D. Lo Presti[1,3], J.R.B. Oliveira[4], P. Finocchiaro[2], M. Colonna[2], D. Rifuggiato[2], L. Calabretta[2], D. Calvo[5], L. Pandola[2], L. Acosta[6], N. Auerbach[7], J. Bellone[1,2], R. Bijker[8], D. Bonanno[3], D. Bongiovanni[2], T. Borello-Lewin[4], I. Boztosun[9], O. Brunasso[5], S. Burrello[2,10], S. Calabrese[1,2], A. Calanna[2], E.R. Chávez Lomelí[6], G. D'Agostino[1,2], P.N. De Faria[11], G. De Geronimo[12], F. Delaunay[5,13], N. Deshmukh[2], J.L. Ferreira[11], M. Fisichella[5], A. Foti[3], G. Gallo[1,2], H. Garcia-Tecocoatzi[14,25], V. Greco[1,2], A. Hacisalihoglu[2,15], F. Iazzi[5,16], R. Introzzi[5,16], G. Lanzalone[2,17], J.A. Lay[2,10], F. La Via[18], H. Lenske[19], R. Linares[11], G. Litrico[2], F. Longhitano[3], J. Lubian[11], N.H. Medina[4], D.R. Mendes[11], M. Moralles[20], A. Muoio[2], A. Pakou[21], H. Petrascu[22], F. Pinna[5,16], S. Reito[3], A.D. Russo[2], G. Russo[1,3], G. Santagati[2], E. Santopinto[14], R.B.B. Santos[23], O. Sgouros[2,21], M.A.G. da Silveira[23], S.O. Solakci[9], G. Souliotis[24], V. Soukeras[2,21], A. Spatafora[1,2], D. Torresi[2], R. Magana Vsevolodovna[14,25], A. Yildirim[9], and V.A.B. Zagatto[11]

Thank you!

Working group

NUMEN Colaboration

J. Lubian, E. N. Cardozo, M. Ermamatov, D. Mendes Jr., R. Linares, B. Paes, V. Zagatto.
Instituto de Fisica, Universidade Federal Fluminense, Niterói, RJ, Brazil

F. Cappuzzello, C. Agodi, D. Carbone, M. Cavallaro and their group at LNS of Catania

Dipartimento di Fisica e Astronomia, Università degli Studi di Catania, Italy
Istituto Nazionale di Fisica Nucleare – Laboratori Nazionali del Sud, Italy
Istituto Nazionale di Fisica Nucleare – Sezione di Catania, Italy

A. Gargano
Istituto Nazionale di Fisica Nucleare – Sezione di Napoli, Italy

E. Santopinto, R. Magana
Istituto Nazionale di Fisica Nucleare – Sezione di Genova, Italy

J. Zamora
INCL- Michigan State Univ., USA

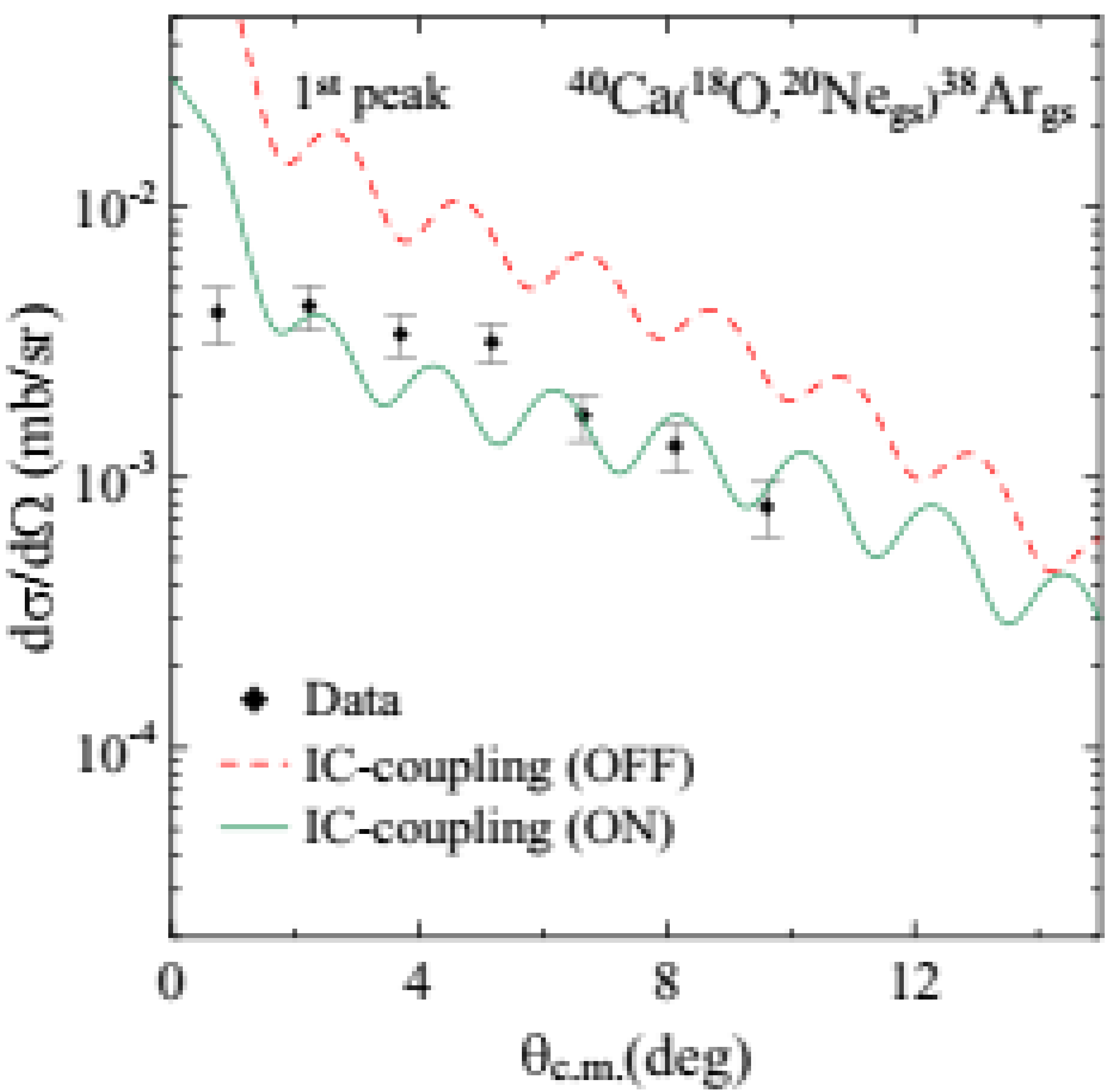
1st peak
40Ca(18O,20Negs)38Args
dσ/dΩ (mb/sr)
10-2
10-3
10-4
Data
IC-coupling (OFF)
IC-coupling (ON)
0
4
8
12
θc.m.(deg)

TABLE IV. Integrated cross sections in the angular range of $0^\circ \leqslant \theta_{c.m.} \leqslant 12^\circ$ for each channel that might contribute to the experimental cross section calculated by direct (IC) and sequential (Seq) mechanisms (see the text). For the fourth peak the cross sections obtained by the ZBM2-modified and *vpth* interactions are listed.

Channels corresponding to the third peak [Fig. 3(a)]

Final channel	Theoretical cross sections (nb)	
	Direct (IC)	Seq
$^{20}Ne_{g.s.}(0^+) + {}^{38}Ar_{3.38}(0^+)$	4.85	6.77
$^{20}Ne_{g.s.}(0^+) + {}^{38}Ar_{3.81}(3^-)$	24.11	29.37
$^{20}Ne_{g.s.}(0^+) + {}^{38}Ar_{3.94}(2^+)$	260.26	317.78
$^{20}Ne_{g.s.}(0^+) + {}^{38}Ar_{4.57}(2^+)$	605.31	694.32
$^{20}Ne_{g.s.}(0^+) + {}^{38}Ar_{4.59}(5^-)$	4.81	9.37
$^{20}Ne_{1.63}(2^+) + {}^{38}Ar_{2.17}(2^+)$	122.60	399.85
$^{20}Ne_{4.25}(4^+) + {}^{38}Ar_{g.s.}(0^+)$	146.90	228.53

Channels corresponding to the fourth peak [Fig. 3(b)]

Final channel	Theoretical cross sections (nb)			
	ZBM2mod		*vpth*	
	IC	Seq.	IC	Seq.
$^{20}Ne_{g.s.}(0^+) + {}^{38}Ar_{5.60}(2^+)$	171.49	614.25	3.09	1.19
$^{20}Ne_{g.s.}(0^+) + {}^{38}Ar_{5.66}(5^-)$	126.54	438.29	44.81	143.44
$^{20}Ne_{g.s.}(0^+) + {}^{38}Ar_{5.83}(3^-)$	71.34	262.76	6.10	12.53
$^{20}Ne_{g.s.}(0^+) + {}^{38}Ar_{6.05}(4^+)$	0.65	0.88	0.0082	0.11
$^{20}Ne_{g.s.}(0^+) + {}^{38}Ar_{6.25}(2^+)$	81.33	242.65	3.95	6.95
$^{20}Ne_{g.s.}(0^+) + {}^{38}Ar_{6.28}(4^+)$	0.28	0.29	0.0402	0.0414
$^{20}Ne_{g.s.}(0^+) + {}^{38}Ar_{6.41}(6^+)$	0.20	2.20	0.0439	0.0032
$^{20}Ne_{g.s.}(0^+) + {}^{38}Ar_{6.52}(2^+)$	115.17	391.42	1.74	0.27
$^{20}Ne_{g.s.}(0^+) + {}^{38}Ar_{6.67}(5^-)$	0.21	4.92	3.51	1.32
$^{20}Ne_{1.63}(2^+) + {}^{38}Ar_{3.94}(2^+)$	1283	2630	7210	7890
$^{20}Ne_{1.63}(2^+) + {}^{38}Ar_{4.57}(2^+)$	3116	8070	28.35	25.03
$^{20}Ne_{1.63}(2^+) + {}^{38}Ar_{4.59}(5^-)$	20.55	58.97	0.98	5.68
$^{20}Ne_{1.63}(2^+) + {}^{38}Ar_{4.88}(3^-)$	178.81	456.11	122.31	50.72
$^{20}Ne_{1.63}(2^+) + {}^{38}Ar_{5.16}(2^+)$	1678	4670	14.06	4.36
$^{20}Ne_{1.63}(2^+) + {}^{38}Ar_{5.35}(4^+)$	3.62	6.88	0.0015	0.0273
$^{20}Ne_{1.63}(2^+) + {}^{38}Ar_{5.51}(3^-)$	34.68	58.61	14.11	7.29
$^{20}Ne_{4.25}(4^+) + {}^{38}Ar_{2.17}(2^+)$	47.33	258.80	78.57	82.14

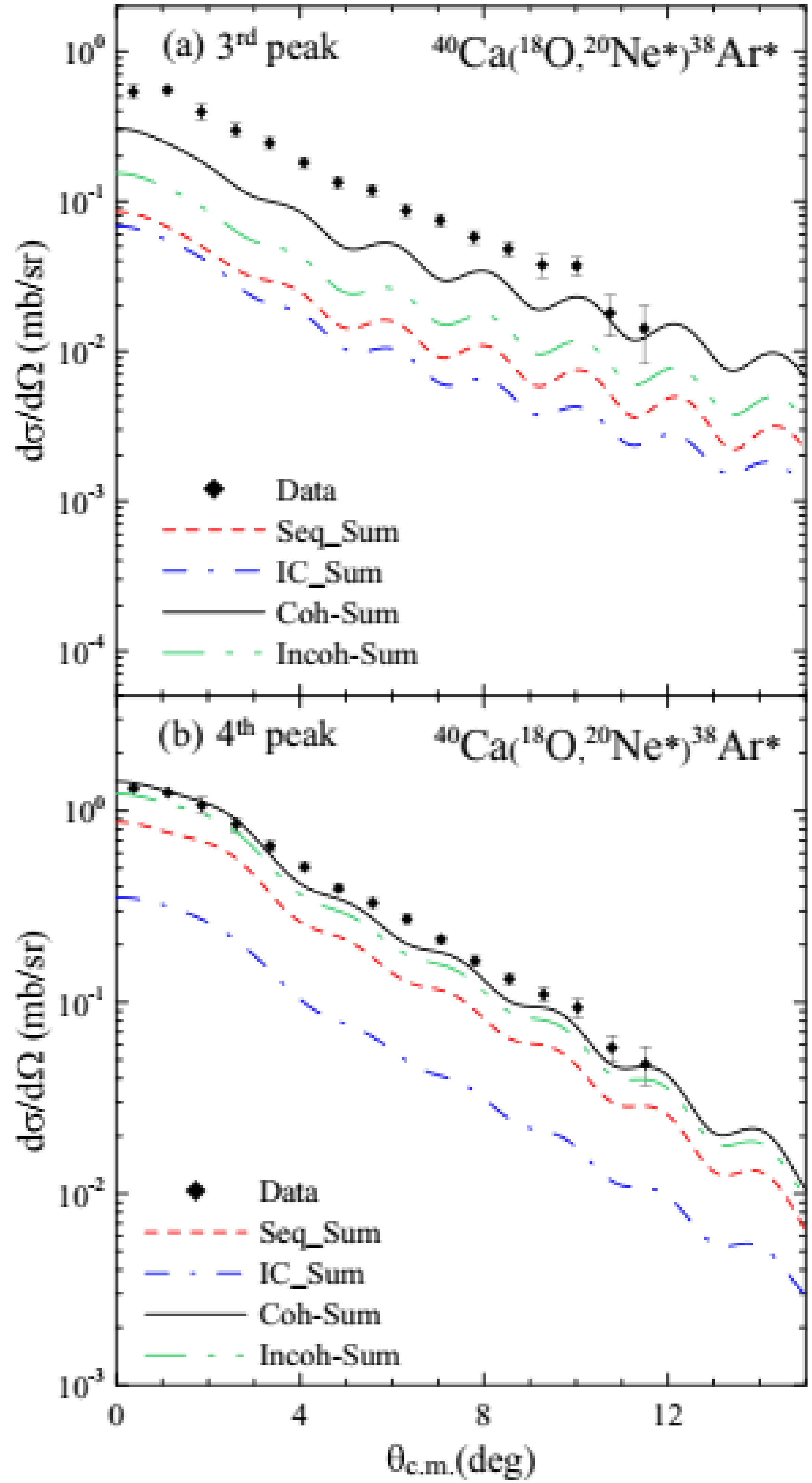

TABLE II. Comparison between the experimental and the theoretical predictions of the reduced electric quadrupole [$B(E2)$] and octupole [$B(E3)$] transition probabilities for the ^{38}Ar, ^{39}K, and ^{40}Ca nuclei.

	^{40}Ca		
$B(E2)$ (e^2fm^4)	$I_i^\pi \rightarrow I_f^\pi$	Exp.	Theo.
	$0_1^+ \rightarrow 2_1^+$	99[a]	105
$B(E3)$ (e^2fm^6)	$I_i^\pi \rightarrow I_f^\pi$	Exp.	Theo.
	$0_1^+ \rightarrow 3_1^-$	11.800[b]	11.420
	^{39}K		
$B(E2)$ (e^2fm^4)	$I_i^\pi \rightarrow I_f^\pi$	Exp.	Theo.
	$1/2_1^+ \rightarrow 3/2_1^+$	6.9[f]; 22[e]	27.4
$B(E3)$ (e^2fm^6)	$I_i^\pi \rightarrow I_f^\pi$	Exp.	Theo.
	$3/2_1^+ \rightarrow 7/2_1^-$	124[f]	106
	$3/2_1^+ \rightarrow 3/2_1^-$	269[f]	217
	$3/2_1^+ \rightarrow 9/2_1^-$	694[f]	90
	$3/2_1^+ \rightarrow 5/2_1^-$	549[f]	1233
	^{38}Ar		
$B(E2)$ (e^2fm^4)	$I_i^\pi \rightarrow I_f^\pi$	Exp.	Theo.
	$0_1^+ \rightarrow 2_1^+$	130[a];121 ± 7.6[d,e]	228.5
	$0_2^+ \rightarrow 2_1^+$	10.63 ± 0.76[e]	15.29
	$0_1^+ \rightarrow 2_2^+$	42[d]	11.43
	$2_1^+ \rightarrow 2_2^+$	56 ± 11[e]	241.9
	$4_1^+ \rightarrow 2_1^+$	7.59 ± 2.28[e]	13.5
	$4_1^+ \rightarrow 2_2^+$	235.3 ± 68.3[e]	41.1
	$6_2^+ \rightarrow 4_1^+$	607 ± 304[e]	37.26
	$5_1^- \rightarrow 3_1^-$	1.44 ± 0.15[e]	
	$5_2^- \rightarrow 3_1^-$	22 ± 5.3[e]	
$B(E3)$ (e^2fm^6)	$I_i^\pi \rightarrow I_f^\pi$	Exp.	Theo.
	$0_1^+ \rightarrow 3_1^-$	9500[b]	1251

[a]Reference [71].
[b]Reference [72].
[c]Reference [75].
[d]Reference [76].
[e]Reference [77].
[f]Reference [78].

TABLE I. Comparison among the ^{38}Ar, ^{39}K, ^{40}Ca experimental spectra, and the one obtained by shell-model calculation considering the ZBM2-modified interaction.

	^{40}Ca	
I^π	$E_{\text{Exp.}}$ (MeV)	$E_{\text{Theo.}}$ (MeV)
0_1^+	0	0
0_2^+	3.353	3.538
3_1^-	3.737	4.614
2_1^+	3.904	4.117
	^{39}K	
I^π	$E_{\text{Exp.}}$ (MeV)	$E_{\text{Theo.}}$ (MeV)
$3/2_1^+$	0	0
$1/2_1^+$	2.523	1.998
$7/2_1^-$	2.814	2.119
$3/2_1^-$	3.019	3.196
$9/2_1^-$	3.597	3.544
$5/2_1^-$	3.883	4.106
$3/2_2^+$	3.939	4.469
$11/2_1^-$	3.944	3.314
$3/2_2^-$	4.082	4.363
$1/2_2^+$	4.096	4.718
$7/2_2^-$	4.127	3.935
	^{38}Ar	
I^π	$E_{\text{Exp.}}$ (MeV)	$E_{\text{Theo.}}$ (MeV)
0_1^+	0	0
2_1^+	2.168	2.201
0_2^+	3.378	3.862
3_1^-	3.810	3.135
2_2^+	3.936	3.418
2_3^+	4.565	4.328
5_1^-	4.586	3.731
3_2^-	4.877	4.782
2_4^+	5.157	4.813
4_1^+	5.349	4.405
3_2^-	5.513	5.224
2_5^+	5.595	5.340
5_2^-	5.659	5.271
3_3^-	5.825	5.631
4_2^+	6.053	5.420
2_6^+	6.250	5.560
4_3^+	6.276	6.071
6_1^+	6.409	5.120
2_7^+	6.520	6.184
5_3^-	6.674	6.227
6_2^+	7.289	6.355

TABLE III. Comparison between the theoretical and experimental low-lying spectra obtained by shell-model calculations for the target and residual nuclei involved in the studied reactions. Energies are in MeV.

Shell model: jj45pna interaction								
^{116}Cd	Expt.	Th.	^{115}Cd	Expt.	Th.	^{114}Cd	Expt.	Th.
0+	0	0	1/2+	0	0.325	0+	0	0
2+	0.513	0.740	(11/2)−	0.181	2.195	2+	0.558	0.604
2+	1.213	1.782	(3/2)+	0.229	0.0	0+	1.135	1.264
4+	1.219	1.712	(5/2)+	0.361	0.534	2+	1.210	1.074
0+	1.283	1.526	(7/2)−	0.394	1.879	4+	1.284	1.543
0+	1.380	2.949	(9/2)−	0.417	2.141	0+	1.305	2.117
Shell model: 88Sr45 interaction								
^{116}Cd	Expt.	Th.	^{117}In	Expt.	Th.	^{118}Sn	Expt.	Th.
0+	0	0	9/2+	0	0	0+	0	0
2+	0.513	0.721	1/2−	0.315	0.078	2+	1.230	0.802
2+	1.213	1.284	3/2−	0.589	1.023	0+	1.758	3.474
4+	1.219	1.653	3/2+	0.660	2.147	2+	2.043	2.018
0+	1.283	2.032	7/2+	0.748	1.082	0+	2.057	4.304
0+	1.380	2.745	1/2+	0.749	2.011	4+	2.280	2.936

TABLE IV. Comparison between calculated and experimental low-lying states for the ^{116}Cd, ^{114}Cd, and ^{118}Sn nuclei. Energies are in MeV.

Interacting Boson Model-2								
^{116}Cd	Expt.	Th.	^{114}Cd	Expt.	Th.	^{118}Sn	Expt.	Th.
0+	0	0	0+	0	0	0+	0	0
2+	0.513	0.516	2+	0.558	0.492	2+	1.230	1.201
2+	1.213	1.178	0+	1.135	1.274	0+	1.758	1.790
4+	1.219	1.186	2+	1.210	1.125	2+	2.043	2.261
0+	1.283	1.325	4+	1.284	1.130	4+	2.280	2.267

TABLE VII. Comparison between experimental and theoretical integrated cross sections corresponding to the two-proton stripping (for $4^\circ < \theta_{\mathrm{lab}} < 14^\circ$) transfer processes. The amplitudes for the projectile overlaps were derived by shell-model calculation using the *p-sd*-mod interaction. For the target overlaps, the results using the jj45pna and 88Sr45 interactions within the SM, microscopic IBM-2, and the QRPA are reported.

		Cross Sections (nb)								
		Theory								
		SA-shell model *p-sd-mod* + *jj45pna* int.				SA-shell model *p-sd-mod* + *88Sr45*		SA IBM-2		SA QRPA
Final Channel	Expt.	IC CRC-1	Seq DWBA	IC CRC-2	Seq CCBA	IC CRC-2	Seq CCBA	IC CRC-1	IC CRC-2	IC CRC-1
$^{18}\mathrm{O}_{\mathrm{gs}}(0^+) + {}^{118}\mathrm{Sn}_{\mathrm{gs}}(0^+)$	40 ± 15	22	19.1	30.9	52.1	39.5	88.5	32.7	23.1	19
$^{18}\mathrm{O}_{\mathrm{gs}}(0^+) + {}^{118}\mathrm{Sn}_{1.229}(2^+)$	140 ± 60	5.3	1.6	26.9	39.8	52.7	106.3	3.1	2.6	55

2n-transfer reactions

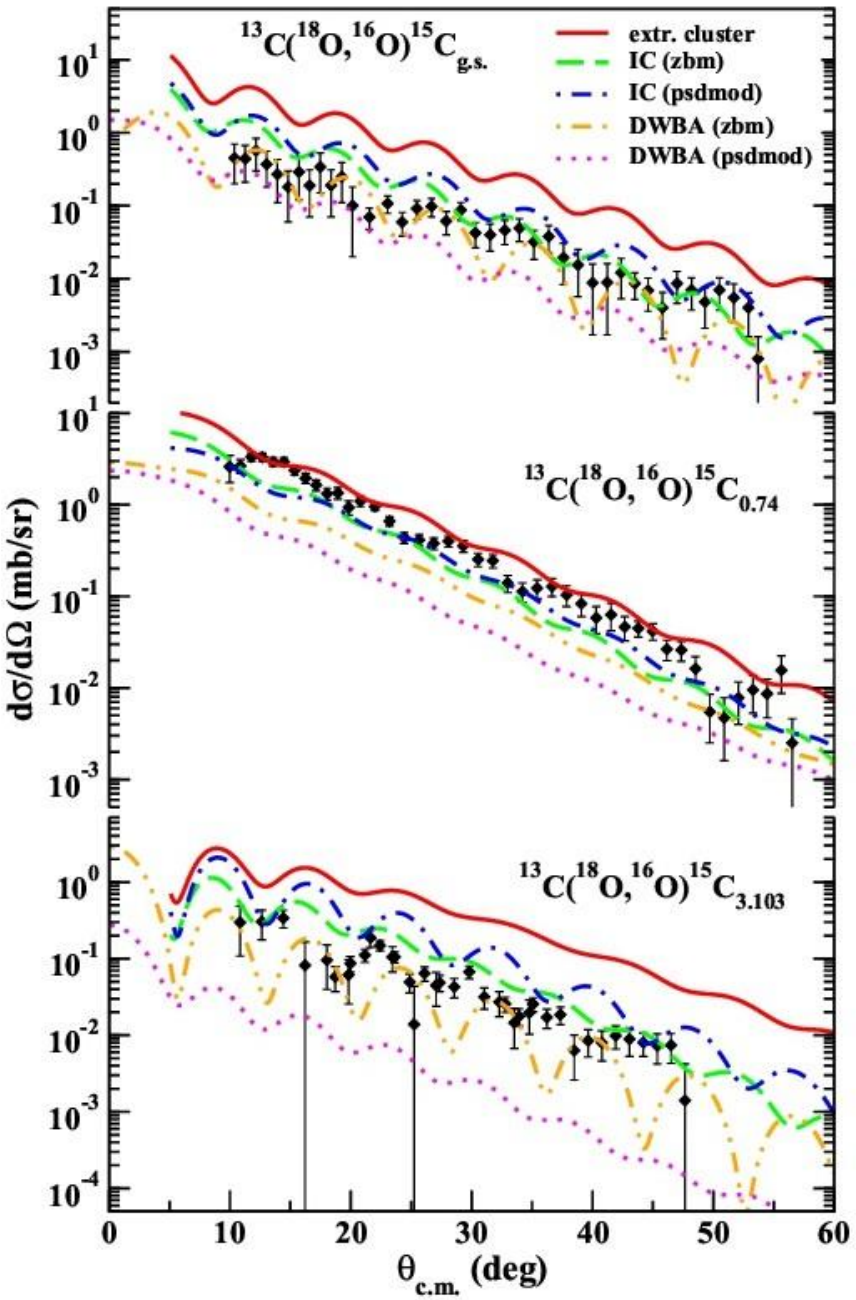

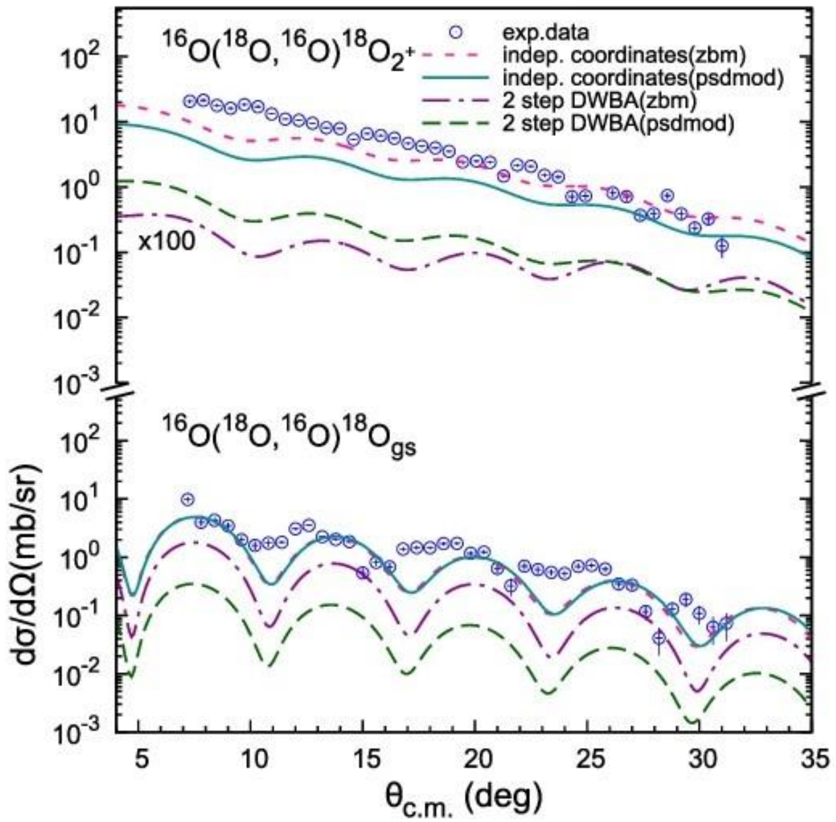

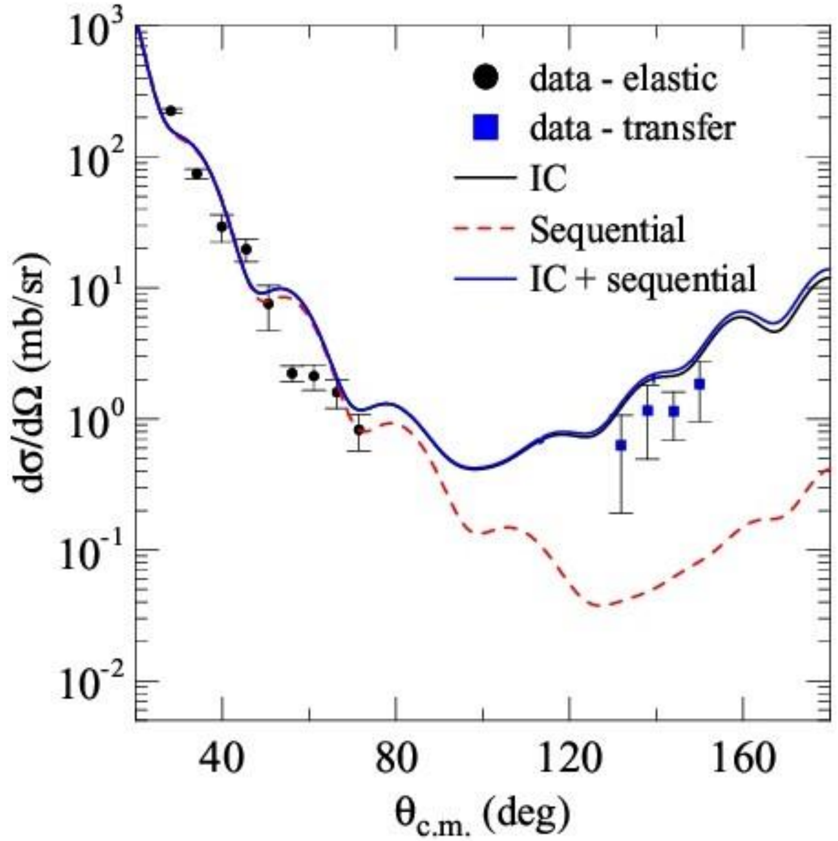

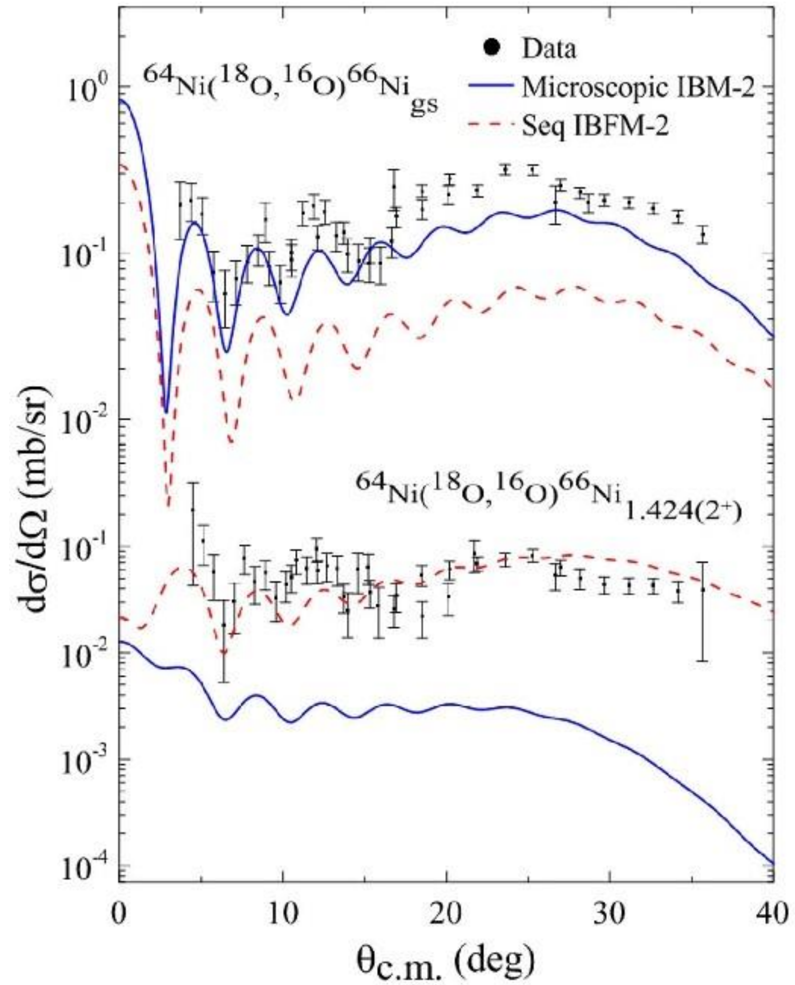

- $^{18}O + ^{13}C$ ➢ **Phys. Rev C 95, 034603 (2017)**
- $^{18}O + ^{16}O$ ➢ **Phys. Rev C 94, 024610 (2016)**
- $^{18}O + ^{16}O$ ➢ **Phys. Rev C 96, 044603 (2017)**
- $^{18}O + ^{64}Ni$ ➢ **Phys. Rev C 96, 044612 (2017)**
- $^{18}O + ^{28}Si$ ➢ **Phys. Rev C 97, 064611 (2018)**
- $^{7}Be + ^{9}Be$ ➢ **Phys. Rev C 99, 064617 (2019)**

Reação de Transferência 1n-transfer

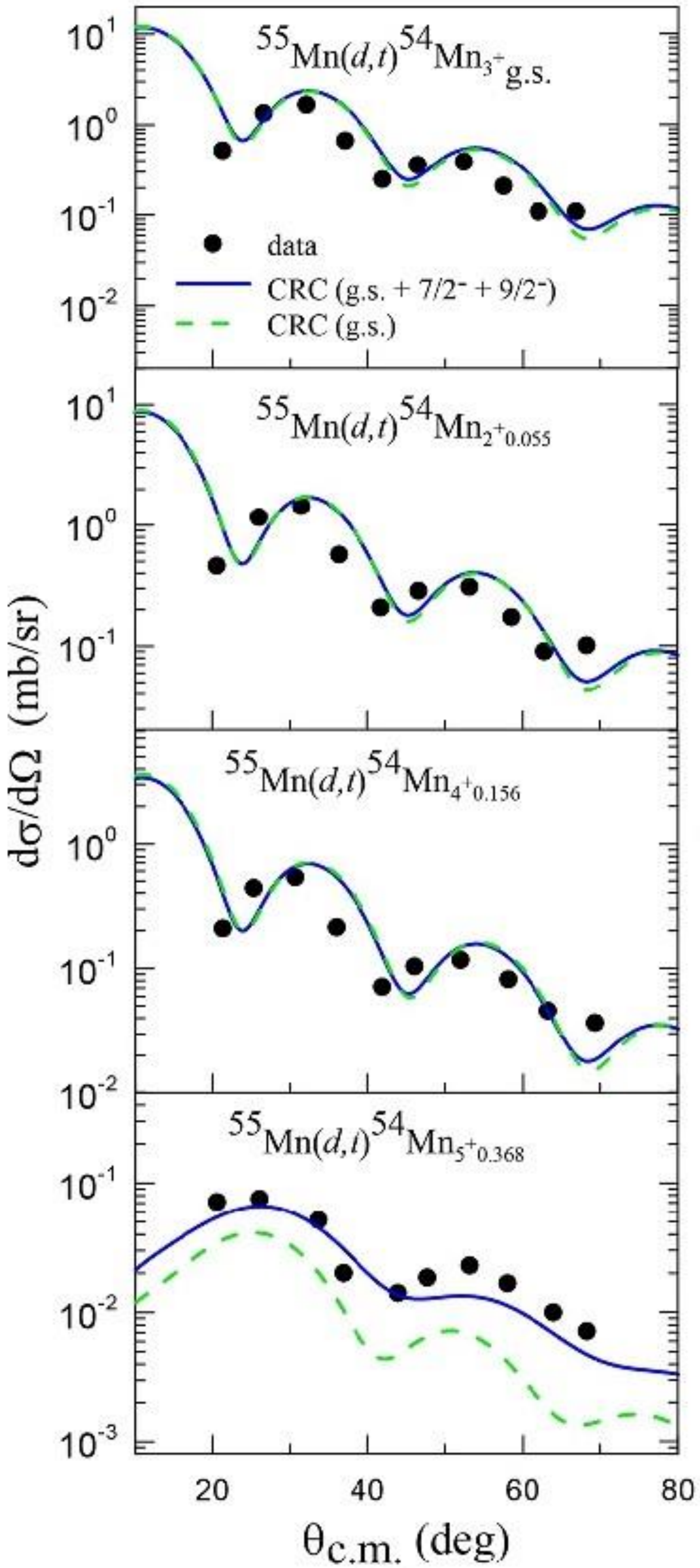

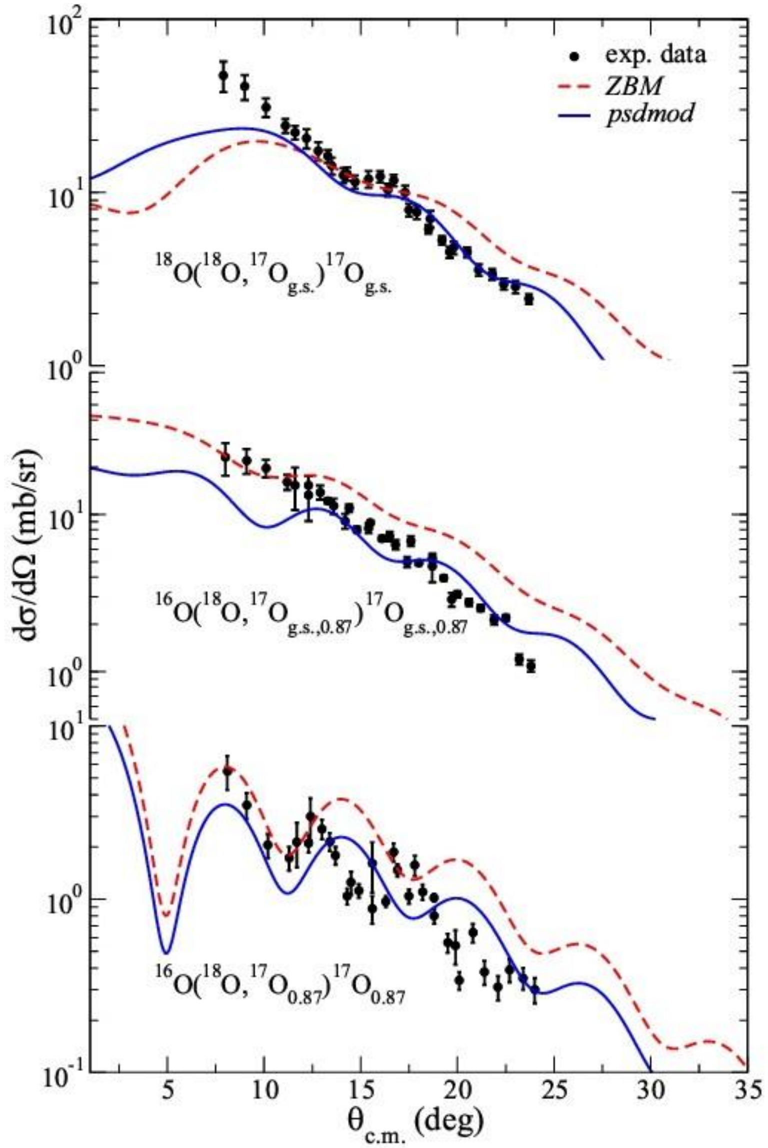

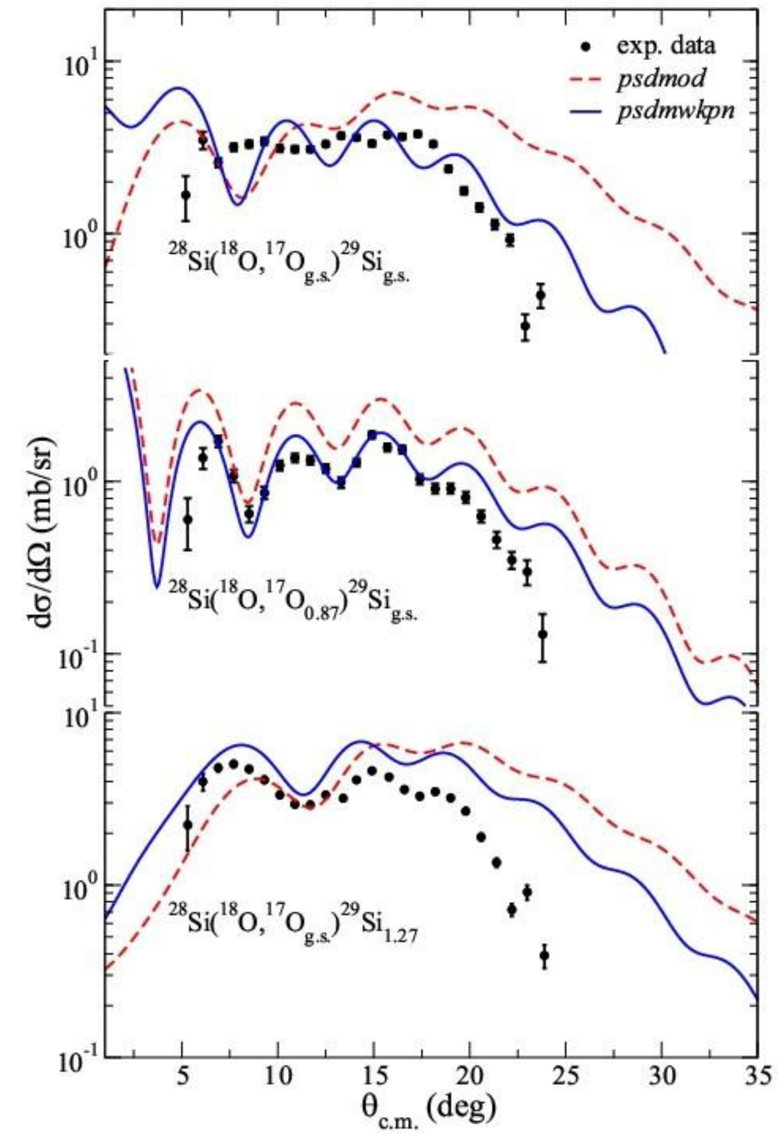

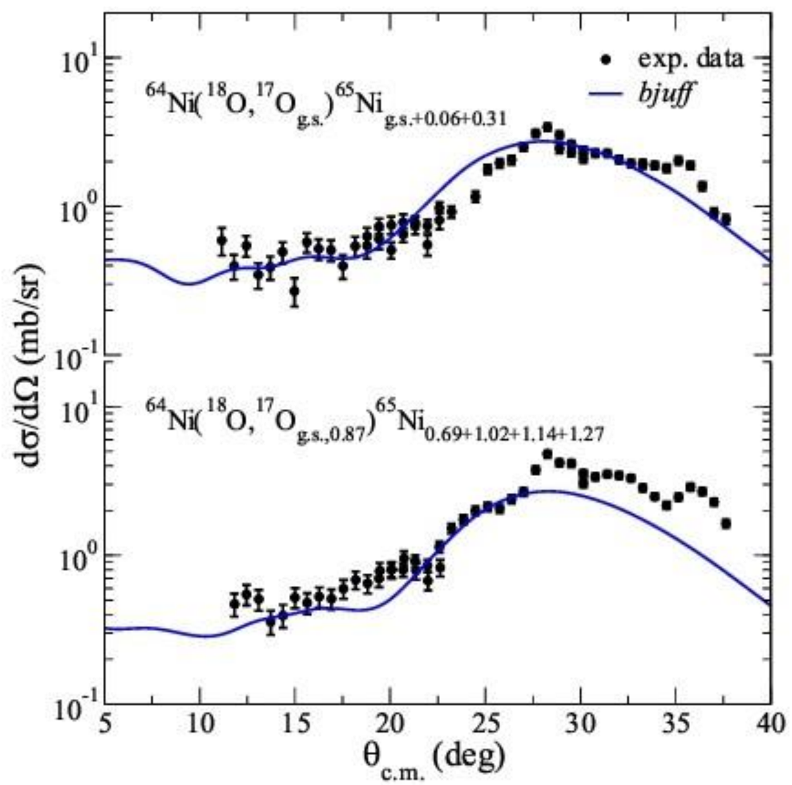

- **Eur. Phys. J. A (2018) 54: 150** — $d + {}^{55}Mn$
- **Phys. Rev C 98, 054615 (2018)** — $^{18}O + {}^{16}O$; $^{18}O + {}^{28}Si$; $^{18}O + {}^{64}Ni$

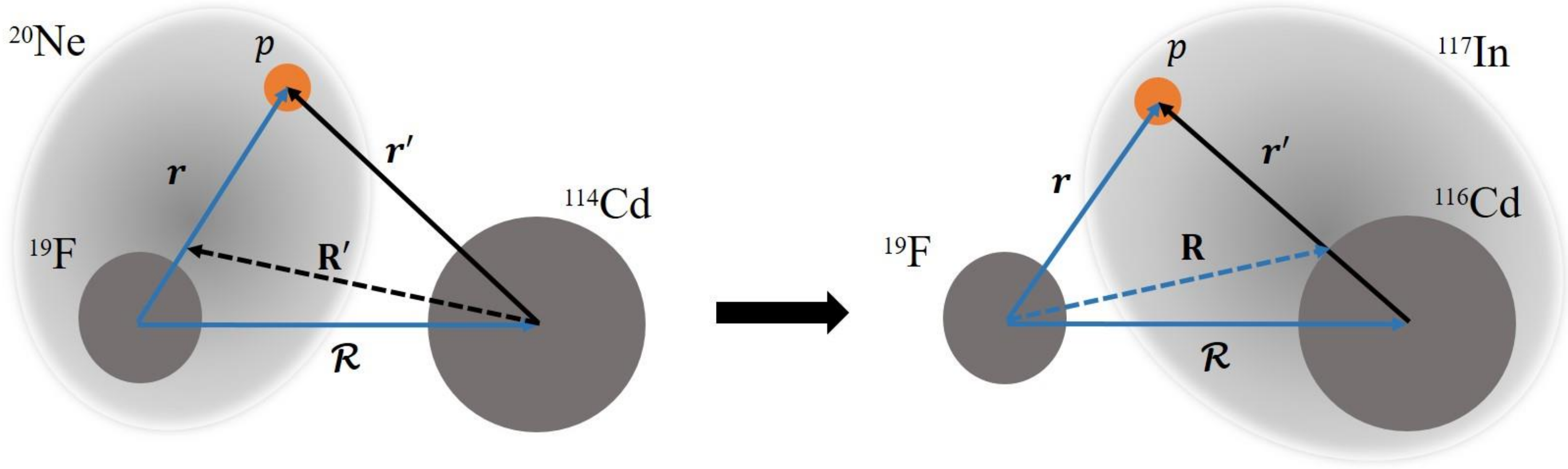

$$\mathrm{H} = T_\alpha + h_\alpha + V_\alpha = T_\beta + h_\beta + V_\beta \quad (1)$$

$$\Psi = \phi_\alpha(\xi_\alpha)\psi_\alpha(\boldsymbol{R}_\alpha) + \phi_\beta(\xi_\beta)\psi_\beta(\boldsymbol{R}_\beta) \quad (2)$$

$$(E_\alpha - T_\alpha - h_\alpha - V_\alpha)\Psi = 0 \quad (3)$$

$$(E - T_\alpha - \varepsilon_\alpha - V_{\alpha\alpha})\psi_\alpha(\boldsymbol{k}_\alpha, \boldsymbol{R}_\alpha) = (E - T_\alpha - \varepsilon_\alpha) n_{\alpha\beta}\psi_\beta(\boldsymbol{k}_\beta, \boldsymbol{R}_\beta) + V_{\alpha\beta}\psi_\beta(\boldsymbol{k}_\beta, \boldsymbol{R}_\beta) \quad (4)$$

$$(E - T_\beta - \varepsilon_\beta - V_{\beta\beta})\psi_\beta(\boldsymbol{k}_\beta, \boldsymbol{R}_\beta) = (E - T_\beta - \varepsilon_\beta) n_{\beta\alpha}\psi_\alpha(\boldsymbol{k}_\alpha, \boldsymbol{R}_\alpha) + V_{\beta\alpha}\psi_\alpha(\boldsymbol{k}_\alpha, \boldsymbol{R}_\alpha) \quad (5)$$

$$n_{\alpha\beta} = \int \phi_\alpha^*(\xi_\alpha)\phi_\beta(\xi_\beta)\, d\xi_\alpha \qquad V_{\alpha\beta} = \int \phi_\alpha^*(\xi_\alpha) V_\alpha \phi_\beta(\xi_\beta)\, d\xi_\alpha \quad (6)$$

NUMEN project

- **Reactions purposed:**
  - $^{40}Ca(^{18}O,^{18}Ne)^{40}Ar$;
  - $^{116}Sn(^{18}O,^{18}Ne)^{116}Cd$;
  - $^{116}Cd(^{18}O,^{18}Ne)^{116}Sn$;
  - $^{116}Cd(^{20}Ne,^{20}O)^{116}Sn$;
  - $^{130}Te(^{20}Ne,^{20}O)^{116}Xe$;
  - $^{76}Ge(^{20}Ne,^{20}O)^{76}Se$;
  - $^{76}Se(^{18}O,^{18}Ne)^{76}Ge$;

A reação $^{116}Cd(^{20}Ne,^{20}O)^{116}Sn$

Mesured Channels

DCE

- ✓ $^{116}Cd(^{20}Ne,^{20}O_{gs})^{116}Sn_{gs}$
- ✓ $^{116}Cd(^{20}Ne,^{20}O_{gs})^{116}Sn_{2+}$

  \+

  $^{116}Cd(^{20}Ne,^{20}O_{2+})^{116}Sn_{gs}$

2p-transfer

- ✓ $^{116}Cd(^{20}Ne,^{18}O_{gs})^{118}Sn_{gs}$
- ✓ $^{116}Cd(^{20}Ne,^{18}O_{gs})^{118}Sn_{2+}$

2n-transfer

- ✓ $^{116}Cd(^{20}Ne,^{22}Ne_{gs})^{114}Cd_{gs}$
- ✓ $^{116}Cd(^{20}Ne,^{22}Ne_{gs})^{114}Cd_{2+}$

Análise da transferência de múltiplos na reação $^{116}Cd(^{20}Ne,^{20}O)^{116}Sn$

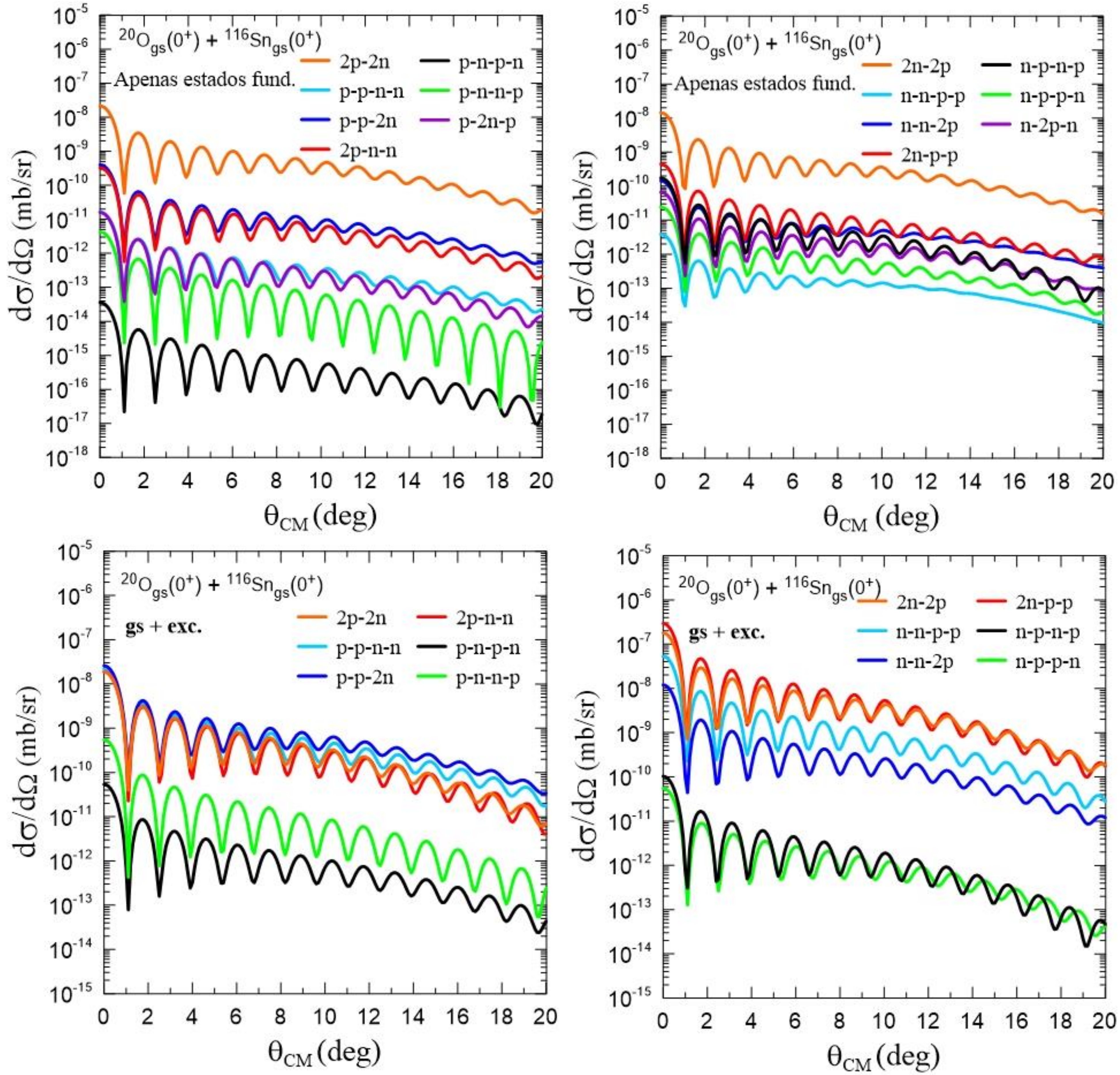

Nucleus	B(E2); $0^+ \rightarrow 2^+$ (e^2b^2)
^{14}C	0.0018
^{18}O	0.0045
^{28}Mg	0.035
^{30}Si	0.022
^{66}Ni	0.060
^{76}Ge	0.270